THE UNIVERSITY of EDINBURGH

Edinburgh Research Explorer

Small x resummation with quarks: Deep-inelastic scattering

OPEN ACCESS

Small x Resummation with Quarks: Deep-Inelastic Scattering

Guido Altarelli,[a, b] Richard D. Ball[c, b] and Stefano Forte[d]

[a] *Dipartimento di Fisica "E.Amaldi", Università Roma Tre*
INFN, Sezione di Roma Tre
Via della Vasca Navale 84, I–00146 Roma, Italy

[b] *CERN, Department of Physics, Theory Division*
CH-1211 Genève 23, Switzerland

[c] *School of Physics, University of Edinburgh*
Edinburgh EH9 3JZ, Scotland

[d] *Dipartimento di Fisica, Università di Milano and*
INFN, Sezione di Milano, Via Celoria 16, I-20133 Milan, Italy

Abstract

We extend our previous results on small-x resummation in the pure Yang–Mills theory to full QCD with n_f quark flavours, with a resummed two-by-two matrix of resummed quark and gluon splitting functions. We also construct the corresponding deep–inelastic coefficient functions, and show how these can be combined with parton densities to give fully resummed deep–inelastic structure functions F_2 and F_L at the next-to-leading logarithmic level. We discuss how this resummation can be performed in different factorization schemes, including the commonly used $\overline{\text{MS}}$ scheme. We study the importance of the resummation effects by comparison with fixed-order perturbative results, and we discuss the corresponding renormalization and factorization scale variation uncertainties. We find that for x below 10^{-2} the resummation effects are comparable in size to the fixed order NNLO corrections, but differ in shape. We finally discuss the phenomenological impact of the small–x resummation, specifically in the extraction of parton distribution from present day experiments and their extrapolation to the kinematics relevant for future colliders such as the LHC.

arXiv:0802.0032v1 [hep-ph] 31 Jan 2008

1. Introduction

The main motivation behind the recent progress in higher order calculations in perturbative QCD is the need of accurate phenomenology at hadron colliders, and in particular the LHC. Therefore, the interest of such calculations lies mostly in their ability to actually lead to an improvement in the accuracy of theoretical predictions of measurable processes. The frontier of present-day perturbative calculations is the next-to-next-to leading (NNLO) order, thanks to the recent determination of three–loop splitting functions [1] as well as the hard partonic cross sections for several processes [2] (for recent results see, for example, [3,4]). However, perturbative evolution at NNLO is unstable in the high energy (small x limit): the size of the NNLO corrections diverges as $x \to 0$ at fixed scale.

The fact that at high energy corrections to perturbative evolution and to hard cross sections are potentially large has been known for a long time (see *e.g.* Ref. [5]). However, even though the study of the leading high energy corrections [6] and their inclusion in perturbative anomalous dimensions [7] has a rather long history, it is only over the last few years that a fully resummed approach to perturbative evolution has been constructed [8,9], mostly stimulated by the availability of deep–inelastic data at very high energy from the HERA collider [10]. In fact, it turns out that even though at fixed perturbative order corrections are very large at small x, their full resummation leads to a considerable softening of small x terms, consistent with the fact that the data do not show any large departure from next-to-leading (NLO) order predictions. However, in order to obtain the resummed results one must include several classes of subleading terms, motivated by various physical constraints, such as momentum conservation, renormalization group invariance and gluon exchange symmetry. The existing approaches to this resummation, as discussed respectively in refs. [8,11–15] and [9,16–19] (see also ref. [20]) though rather different in many technical respects, are essentially based on the same physical input and yield results which agree with each other within the expected theoretical uncertainty.

Because the leading high energy corrections are dominated by gluon exchange, the resummation is most easily performed in the pure Yang-Mills theory, and indeed the fully resummed results for perturbative evolution of refs. [8,9,11–19] have been obtained with $n_f = 0$. In order to actually get predictions for (flavour singlet) physical observables, one needs to combine three ingredients: the eigenvalues of the singlet quark and gluon anomalous dimension matrix, the resummed partonic cross sections (coefficient functions) for the relevant physical process in some factorization scheme, and the linear transformation which relates the eigenvectors of the evolution matrix to the singlet quark and the gluon in the same factorization scheme. The first ingredient is readily available: because the effect of one of the two evolution eigenvalues is suppressed by a power of x at small x, it is enough to generalize the results of refs. [8-19] for the "large" eigenvalue to the case $n_f \neq 0$. The second ingredient is also available, at least for a small number of processes [21–23] for which the high–energy resummation of partonic cross sections has been performed. In particular, deep–inelastic coefficient functions have been determined in the $\overline{\text{MS}}$ and DIS (and related) schemes in ref. [22]. However, it is nontrivial to combine resummed coefficient functions and parton distributions at the running coupling level: the way to do this has only been recently developed in ref. [24]. Hence, in order to obtain complete results what we need is to construct the evolution eigenvectors in terms of quarks and gluons at the

resummed level in these schemes. This can be done by extending to the running coupling case the general technique for the construction of resummed factorization schemes which was developed in refs. [12,25].

In this paper, we will present a construction of resummed physical observables in the $\overline{\text{MS}}$ and related schemes, based on the approach to resummation of refs. [8,11-15], using the strategy that we just outlined, and apply it to the specific case of deep–inelastic scattering. We start by summarising the results on small x resummation of singlet evolution developed in previous papers for the pure Yang-Mills theory. We then construct the two eigenvalues of the anomalous dimension matrix when $n_f \neq 0$, by a suitable generalization of the technique of ref. [15]. Next, we show how the deep–inelastic structure functions $F_2(x, Q^2)$ and $F_L(x, Q^2)$ can be obtained by combining resummed coefficient functions with parton distributions which satisfy resummed evolution equations, exploiting the recent results of ref. [24]. Then, we construct the transformation from the basis of eigenvectors of perturbative evolution to that of quarks and gluons in the $\overline{\text{MS}}$ and $\text{Q}_0\overline{\text{MS}}$ schemes and we use it to construct the two-by-two matrix of splitting functions in these schemes. Finally, we discuss the phenomenological consequence of the resummation: first we assess the impact on splitting functions and on the evolution of representative quark and gluon distributions, and then we determine the effect on the deep inelastic structure functions $F_2(x, Q^2)$ and $F_L(x, Q^2)$.

Recently, the full $n_f \neq 0$ resummed evolution matrix has also been constructed explicitly in ref. [26], based on the approach of refs. [9,16-19]. This result has been obtained by extending a BFKL–like approach to coupled quark and gluon evolution. This has the advantage of giving evolution equations for off-shell, unintegrated parton distributions, but it has the shortcoming of providing results in a factorization scheme which only coincides with $\overline{\text{MS}}$ up to the next-to-leading fixed order, and differs from it at the resummed level: it is therefore difficult to compare our results to those of this reference, where no predictions for physical observables are given.

2. Resumming the singlet anomalous dimension matrix

When $n_f \neq 0$, we must consider the full set of splitting functions $P_{ij}(\alpha_s, x)$, where i, j run over quarks, gluons, or linear combinations thereof. However, the resummation of the full set of $P_{ij}(\alpha_s, x)$ can be obtained from the resummation of the largest (gluon-sector) eigenvector of the anomalous dimension matrix

$$\gamma_{ij}(\alpha_s, N) = \int_0^1 dx \, x^{N-1} P_{ij}(\alpha_s, x), \qquad (2.1)$$

as discussed long ago in ref. [12]. The construction of the resummed anomalous dimension when $n_f = 0$ was in turn described in detail in ref. [15]. In this section, we will recall the general structure of the resummation of the large anomalous dimension of ref. [15], concentrating on the aspects which require modification when $n_f \neq 0$, while referring to ref. [15] for details of the resummation.

As is well known, all nonsinglet splitting functions are suppressed by a power of x in comparison to the singlet [27]: namely, the rightmost singularity of γ_{ij} is at $N = 0$ in the

singlet channel and at $N = -1$ in the nonsinglet channel. Therefore we will henceforth only consider the singlet sector, where the anomalous dimension is a two-by-two matrix which provides the evolution of the Mellin moments

$$f(N, t) = \int_0^1 dx\, x^{N-1} f(x, t), \tag{2.2}$$

of the parton distributions

$$f(x, t) = \begin{pmatrix} Q(x, t) \\ G(x, t) \end{pmatrix} = \begin{pmatrix} xq(x, t) \\ xg(x, t) \end{pmatrix}, \tag{2.3}$$

(where q and g are the usual singlet quark and gluon parton densities) according to the evolution equation

$$\frac{d}{dt} f(N, t) = \gamma(\alpha_s(t), N) f(N, t), \tag{2.4}$$

where $t = \ln(Q^2/\mu^2)$. As also well known, the reason why only one of the eigenvalues $\gamma^{\pm}(\alpha_s, N)$ of this matrix needs to be resummed is that only one eigenvalue is nonvanishing at the leading log x (LLx) level, i.e., only one eigenvalue has a k-th order pole at $N = 0$ when evaluated at order α_s^k, so

$$\begin{aligned} \gamma^+_{\mathrm{LL}x}(\alpha_s, N) &= \gamma_s^+ \left(\tfrac{\alpha_s}{N} \right), \\ \gamma^-_{\mathrm{LL}x}(\alpha_s, N) &= 0. \end{aligned} \tag{2.5}$$

It follows that it is possible to choose the factorization scheme in such a way that $\gamma^-(\alpha_s, N)$ is regular at $N = 0$ [12,25]. In particular, this is the case at the next-to-leading log x level in the $\overline{\mathrm{MS}}$ and DIS schemes [22]. We will henceforth only consider schemes where γ^- is regular at $N = 0$, and thus only γ^+ has to be resummed.

2.1. The dominant singlet eigenvector

The resummation of γ^+ is performed as discussed in ref. [15]. In order to understand this resummation, it is useful to recall that the solution of the GLAP equation (2.4) for the large eigenvector f^+ of γ,

$$\frac{d}{dt} f^+(N, t) = \gamma^+(\alpha_s(t), N) f^+(N, t), \tag{2.6}$$

coincides at leading twist with the solution to the BFKL equation

$$\frac{d}{d\xi} f^+(x, M) = \chi(\hat{\alpha}_s, M) f^+(x, M), \tag{2.7}$$

where $\xi = \ln(1/x)$, $f^+(x, M)$ is the Mellin transform

$$f^+(x, M) = \int_{-\infty}^{\infty} dt\, e^{-Mt} f^+(x, t), \tag{2.8}$$

3

$\hat{\alpha}_s$ is the operator obtained from $\alpha_s(t)$ by the replacement $t \to -\frac{\partial}{\partial M}$, and the kernel[1]

$$\chi(\hat{\alpha}_s, M) = \hat{\alpha}_s \chi_0(M) + \hat{\alpha}_s^2 \chi_1(M) + \cdots \tag{2.9}$$

is determined by the kernel γ (or conversely) by a suitable duality relation [29,11,13,28]. Because parton distributions behave as a constant at large Q^2, while they vanish linearly with Q^2 as $Q^2 \to 0$, the integral eq. (2.8) exists when $0 < \text{Re}M < 1$ (physical region, henceforth), and it can be defined elsewhere by analytic continuation.

At fixed coupling the duality relations between the kernels are simply

$$\chi(\alpha_s, \gamma^+(\alpha_s, N)) = N,$$
$$\gamma^+(\alpha_s, \chi(\alpha_s, M)) = M, \tag{2.10}$$

which imply that if we expand $\gamma^+(\alpha_s, N)$ in powers of α_s at fixed α_s/N

$$\gamma^+(\alpha_s, N) = \gamma_s^+(\tfrac{\alpha_s}{N}) + \alpha_s \gamma_{ss}^+(\tfrac{\alpha_s}{N}) + \cdots, \tag{2.11}$$

γ_s^+ is determined by χ_0 (and conversely), γ_{ss}^+ by χ_0 and χ_1 and so on. At the running coupling level it is still true that the first n orders of the expansion eq. (2.11) are determined by $\chi(\alpha_s, M)$, eq. (2.9), up to n-th order, but eq. (2.10) holds only at leading order (i.e. for χ_0 and γ_s), while beyond the leading order it gets corrected by a series of terms up to $O[(\beta_0\alpha_s)^{n-1}]$, which can be determined explicitly order-by-order in perturbation theory [28]. Conversely, the first n orders of the expansion of χ in powers of M at fixed $M^{-1}\hat{\alpha}_s$

$$\chi(\hat{\alpha}_s, M) = \chi_s(M^{-1}\hat{\alpha}_s) + \hat{\alpha}_s \chi_{ss}(M^{-1}\hat{\alpha}_s) + \cdots \tag{2.12}$$

are determined by knowledge up to n-th order of the expansion of γ^+ at fixed N

$$\gamma^+(\alpha_s, N) = \alpha_s \gamma_0^+(N) + \alpha_s^2 \gamma_1^+(N) + \cdots. \tag{2.13}$$

Of course, different orderings of M^{-1} and $\hat{\alpha}_s$ in the argument of the coefficients χ_{s^n} of the expansion eq. (2.12) lead to a different functional form of the coefficients; the ordering eq. (2.12) is particularly convenient because with it the leading order coefficient χ_s has the same form as that obtained from γ_0 using fixed-coupling duality eq. (2.10) [28].

The resummation of $\gamma^+(\alpha_s, N)$ at k-th order consists of supplementing the k-th order of its expansion in powers of α_s eq. (2.13) with three further classes of terms: (a) terms up to k–th order in the expansion of γ^+ in powers of α_s with α_s/N fixed, eq. (2.11), (double-leading resummation, henceforth); (b) contributions which are subleading with respect to the double-leading resummation but which enforce the physical constraints of momentum conservation and gluon exchange symmetry (symmetrization, henceforth); (c) contributions which are subleading with respect to the double-leading expansion but which are needed in order to ensure the uniform convergence of that expansion in the physical

---

[1] Different choices of ordering for the operator $\hat{\alpha}_s$ in the definition of the kernel correspond to different choices for the argument of the running coupling [28].

region (running-coupling resummation, henceforth). Let us now discuss the resummation of these classes of terms in turn.

The double–leading resummation (first step) is performed by combining the first k orders of the expansion of γ^+ in powers of α_s at fixed N eq. (2.13) and at fixed α_s/N eq. (2.11) (double-leading expansion [30,11]), and subtracting double counting:

$$
\begin{aligned}
\gamma_{\mathrm{DL}}^+(N, \alpha_s) = {} & \left[\alpha_s \gamma_0^+(N) + \gamma_s^+\left(\tfrac{\alpha_s}{N}\right) - \tfrac{n_c \alpha_s}{\pi N}\right] \\
& + \alpha_s \left[\alpha_s \gamma_1^+(N) + \gamma_{ss}^+\left(\tfrac{\alpha_s}{N}\right) - \alpha_s \left(\tfrac{e_2^+}{N^2} + \tfrac{e_1^+}{N}\right) - e_0\right] + \cdots.
\end{aligned}
\tag{2.14}
$$

The key observation is that one can prove [11] that the double–leading expansion of γ^+ eq. (2.14) and the double leading expansion of χ are order by order dual to each other. This is crucial because the subsequent steps of the resummation (symmetrization and running-coupling resummation) are performed by manipulating χ. The construction of the resummed γ^+ thus starts [15] by transforming the double–leading $\gamma_{\mathrm{DL}}^+(N, \alpha_s)$ eq. (2.14) into its dual

$$
\begin{aligned}
\chi_{\mathrm{DL}} = {} & \left[\alpha_s \chi_0(M) + \chi_s\left(\tfrac{\alpha_s}{M}\right) - \tfrac{n_c \alpha_s}{\pi M}\right] \\
& + \alpha_s \left[\alpha_s \chi_1(M) + \chi_{ss}\left(\tfrac{\alpha_s}{M}\right) - \alpha_s \left(\tfrac{f_2}{M^2} + \tfrac{f_1}{M}\right) - f_0\right] + \cdots.
\end{aligned}
\tag{2.15}
$$

The kernel χ eq. (2.15) has a stable perturbative expansion for small M. This is a consequence of the fact that momentum conservation implies [12] that $\gamma^+(1) = 0$, which, by duality, entails $\chi(0) = 1$ (up to running coupling corrections). These properties are exactly satisfied order-by-order by the perturbative expansion eq. (2.13) of γ^+, and thus only violated by (small) subleading terms in the double–leading expansion eq. (2.15) of χ, which is thus finite (and close to one) at $M = 0$ despite the fact that subsequent orders of the expansion eq. (2.9) of χ have poles of increasingly high order and alternating sign coefficients: these poles are removed by the double leading resummation eq. (2.15). However, order by order in the expansion eq. (2.9) the kernel χ also has poles at $M = 1$. Hence, the double–leading expansion of χ is still perturbatively unstable when M grows sufficiently large. This is problematic because perturbative evolution at small x is controlled by the small N behaviour of γ^+, which by duality corresponds to the large M behaviour of χ.

This instability can be cured by exploiting a symmetry of the set of Feynman diagrams which determine the kernel χ, that implies that the kernel satisfies the reflection relation $\chi(M) = \chi(1-M)$ order by order in perturbation theory. This exchange symmetry is broken by an asymmetric choice of kinematic variables, as is necessary for the application to deep inelastic scattering, and by running coupling effects [16,18]. The double–leading kernel can thus be symmetrized by first undoing all sources of symmetry breaking, then symmetrizing, and finally restoring the symmetry breaking. The symmetrization must be performed in such a way that the symmetrized kernel χ_Σ only differs from the double-leading χ_{DL} by subleading terms. This introduces a certain ambiguity, which however is controlled by the requirement of momentum conservation, which fixes the value of χ at $M = 0$. The way the symmetrization can be implemented at the leading- and next-to-leading order of the

5

double-leading expansion was described in detail in ref. [15] to which we refer, since the procedure is unchanged regardless of the value of n_f. Once the resummed, symmetrized kernel $\chi_\Sigma(M)$ has been constructed to the desired order, the corresponding resummed anomalous dimension γ_Σ^+ can be obtained from it using running–coupling duality, as we shall see shortly.

An important consequence of the symmetrization of χ is that the symmetrized kernel always has a minimum in the physical region $0 \le \operatorname{Re} M \le 1$, and it is an entire function of M for $\operatorname{Re} M > 0$. The existence of the minimum is a generic consequence of symmetrization of the behaviour around the momentum conservation value $\chi(0) = 1$, where the kernel has negative derivative; this in turn is, by duality, a generic consequence of the physical requirement that γ^+ decreases as N increases. The fact that the kernel is an entire function then follows from the transformation from the kinematics in which the kernel is symmetric (appropriate for processes such as two-jet production in p–p scattering) to that of DIS [15]. The transformation from symmetric to DIS variables leaves unchanged the value of χ at the minimum (and the curvature of χ at the minimum [15]), but shifts the position of the minimum away from $M = \frac{1}{2}$ by small corrections.

The existence of a minimum of χ is what makes the third step, the running-coupling resummation, necessary. Indeed, the double–leading improvement eq. (2.14) of the expansion (2.13) of γ^+ is necessary but not sufficient for the perturbative corrections to γ^+ to be uniformly small in the small x limit: the inclusion of the first k orders of the expansion eq. (2.11) of γ^+ in powers of α_s at fixed α_s/N guarantees that the $O(k+1)$ is $O(\alpha_s)$ if α_s/N is kept fixed as N decreases, but not if N decreases at fixed α_s. Now, if χ has a minimum at $M = M_0$, in the vicinity of the minimum we can expand

$$\chi^q(\hat{\alpha}_s, M) = c(\hat{\alpha}_s) + \tfrac{1}{2}\kappa(\hat{\alpha}_s)\,(M - M_0)^2 + O\left[(M - M_0)^3\right]. \tag{2.16}$$

The fixed–coupling dual to χ^q eq. (2.16) is

$$\gamma_q^+(\alpha_s, N) = M_0 - \sqrt{\frac{N - c(\alpha_s)}{\tfrac{1}{2}\kappa(\alpha_s)}}, \tag{2.17}$$

which has square-root branch cut at $N = \chi^q(\alpha_s, M_0)$. However, the running coupling correction to γ_{ss} in the vicinity of the minimum is

$$\begin{aligned}
\gamma_{ss}^{\beta_0}(\alpha_s, N) &= -\beta_0 \frac{\chi_0''(\gamma_q^+)\chi_0(\gamma_q^+)}{2[\chi_0'(\gamma_q^+)]^2} \\
&= -\frac{1}{4}\beta_0 \frac{N}{N - c(\alpha_s)},
\end{aligned} \tag{2.18}$$

which has a simple pole at $N = \chi(M_0)$.

In general, the running coupling correction to γ_{s^n} has an order n pole at $M = M_0$ [28,31]. This implies the growth of the associated splitting function by a power of $\ln 1/x$ equal to the order of the pole in comparison to a pole–free splitting function. Hence

the running coupling contributions are not uniformly small at small x and they must be resummed.

The resummation of running coupling singularities is possible [13] thanks to the fact that the running-coupling BFKL equation (2.7) can be solved in closed form either for a quadratic kernel which is linear in α_s [32] or, at the leading log level, for a quadratic kernel which is a generic function of α_s. As derived in detail in refs.[14,15], the inverse Mellin transforms of these two closed form solutions can be written down in terms of an Airy function or a Bateman function, $G_A(N,t)$ or $G_B(N,t)$, respectively. It is then possible to determine the associated anomalous dimensions as their logarithmic derivative:

$$\gamma_B(\alpha_s, N) = \frac{\partial}{\partial t} \ln G_B(N,t). \qquad (2.19)$$

The Bateman result includes the Airy case to which it reduces for a kernel which is proportional to α_s.

The "Bateman" anomalous dimension eq. (2.19) resums to all orders the leading singular running coupling corrections to duality. The leading singularity which controls the small x behaviour is then the singularity of the Bateman anomalous dimension, which is a simple pole:

$$\gamma_B(\alpha_s(t), N) = \frac{1}{N - N_0} r_B + O[(N - N_0)^0], \qquad r_B = 2\beta_0\bar{\alpha}_s \left[N_0 - \bar{c}(\alpha_s)\right], \qquad (2.20)$$

where N_0 is related to the location of the zeros of the Bateman function in eq. (2.19). The value of N_0 depends on the values of $c(\alpha_s)$ and $\kappa(\alpha_s)$. It is plotted as a function of $\alpha_s(t)$ at LO and NLO in ref. [15]. Specifically, for $\alpha_s = 0.2$, $N_0 \approx 0.17$ at both LO and NLO. This value corresponds to a drastic suppression of the asymptotic rise at small x with respect to the fixed coupling case. Moreover, the smallness of the associated residue r_B delays the onset of the powerlike asymptotic behaviour to values of x below the region of the HERA data.

A resummed result which is uniformly stable at small x is found by simply combining the anomalous dimension obtained using running coupling duality from the symmetrized kernel χ_Σ with the "Bateman" resummation eq. (2.19) of the running coupling corrections, and subtracting the double counting. Namely, at next-to-leading order, one first constructs

$$\gamma_{\Sigma\,NLO}^{+\,rc,\,pert}(\alpha_s(t), N) = \gamma_{\Sigma\,NLO}^{+}(\alpha_s(t), N) - \beta_0\alpha_s(t) \left[\frac{\chi_0''(\gamma_s^+(\frac{\alpha_s}{N}))\chi_0(\gamma_s^+(\frac{\alpha_s}{N}))}{2[\chi_0'(\gamma_s^+(\frac{\alpha_s}{N}))]^2} - 1\right], \quad (2.21)$$

where $\gamma_{\Sigma\,NLO}^{+}(N, \alpha_s(t))$ is obtained from the NLO symmetrized kernel $\chi_{\Sigma\,NLO}$ using fixed–coupling duality eq. (2.10), and the term proportional to β_0 is the running coupling correction. Then the result is combined with the Bateman resummation:

$$\begin{aligned}
\gamma_{NLO}^{+\,res} \equiv \gamma_{\Sigma\,NLO}^{+\,rc}(\alpha_s(t), N) &= \gamma_{\Sigma\,NLO}^{+\,rc,\,pert}(\alpha_s(t), N) + \gamma^B(\alpha_s(t), N) + \\
&- \gamma_s^B(\alpha_s(t), N) - \gamma_{ss}^B(\alpha_s(t), N) + \gamma_{\text{match}}(\alpha_s(t), N) + \gamma_{\text{mom}}(\alpha_s(t), N),
\end{aligned} \qquad (2.22)$$

7

where the double counting subtractions $\gamma_{B,s}$ and $\gamma_{B,ss}$ are defined from the expansion

$$\gamma_B(\alpha_s, N) = \gamma_{B,s}(\tfrac{\alpha_s}{N}) + \alpha_s \gamma_{B,ss}(\tfrac{\alpha_s}{N}) + O(\alpha_s^2), \tag{2.23}$$

γ_{mom} is a subleading correction which enforces exact momentum conservation, and γ_{match} is a subleading correction which ensures that at large N the resummed result exactly coincides with the unresummed NLO result γ_{NLO}^+ rather than just reducing to it up to NNLO terms, and specifically that all subleading terms induced by the resummation vanish at least as $1/N$ as $N \to \infty$.

2.2. Virtual quark effects

The construction of the resummed anomalous dimension discussed so far is the same as that of ref. [15], the only difference being that when $n_f = 0$ there is only one parton distribution and one anomalous dimension, while when $n_f \neq 0$ the anomalous dimension one resums is the eigenvector γ^+ of the two-by-two singlet anomalous dimension matrix. There is a complication however. Namely, the two eigenvalues of the leading–order anomalous dimension matrix γ_0 become equal at a pair of complex conjugate values $N^d = N_r^d \pm i N_i^d$, with $N_r^d > 0$, where the square root of the discriminant of the quadratic secular equation vanishes, *i.e.* when

$$(\gamma_0^{qq} - \gamma_0^{gg})^2 + 4\gamma_0^{qg}\gamma_0^{gq} = 0. \tag{2.24}$$

Thus when $n_f \neq 0$, γ_0^+ has a pair of branch cuts. These singularities are manifestly unphysical, and indeed they cancel in the solution of the evolution equations. Because they are to the right of $N = 0$, if uncancelled they would lead to a spurious oscillation of the solution to the evolution equations: the splitting function computed as the inverse Mellin transform of γ_0^+ is oscillatory at small x. After resummation, however, the cancellation of singularities can be spoiled by subleading corrections. Even though these corrections are formally subleading, they can lead to large effects due to the small x instabilities they induce. In order to avoid unphysical behaviour of the solutions, we must make sure that the resummation corrections are implemented in such a way that the cancellation of these singularities remains exact in the final solution, which in turn requires that the unphysical branch cuts in the anomalous dimension be identical to those in the fixed order anomalous dimension.

We do this in the following way. Firstly we separate off the n_f dependent resummation correction $\Delta^{\mathrm{res}}\gamma_{NLO}^{+res}$ to the resummed anomalous dimension γ_{NLO}^{+res} eq. (2.22):

$$\gamma_{NLO}^{+res}(\alpha_s, N; n_f) \equiv \gamma_{NLO}^{+res}(\alpha_s, N; 0) + \gamma_{NLO}^{+cut}(\alpha_s, N; n_f) + \Delta\gamma_{NLO}^{+res}(\alpha_s, N; n_f), \tag{2.25}$$

$$\gamma_{NLO}^{+cut}(\alpha_s, N; n_f) \equiv \alpha_s \gamma_0^+(N; n_f) + \alpha_s^2 \gamma_1^+(N, n_f) - (\alpha_s \gamma_0^+(N; 0) + \alpha_s^2 \gamma_1^+(N, 0)), \tag{2.26}$$

where eq. (2.25) can be viewed as a definition of $\Delta\gamma_{NLO}^{+res}$ in terms of γ_{NLO}^{+res}. All the n_f dependence is now made explicit: $\gamma_{NLO}^{+res}(\alpha_s, N; 0)$ is cut free, while $\gamma_{NLO}^{+cut}(\alpha_s, N; n_f)$ contains the fixed order cuts described above, but vanishes at $n_f = 0$. The formally subleading but asymptotically dominant singularities would arise if $\Delta\gamma_{NLO}^{+res}(\alpha_s, N; n_f)$ were calculated using the $n_f \neq 0$ version of eq. (2.22): the cut in γ_{NLO}^{+cut} would propagate into χ_s and thus χ_{DL} eq. (2.15). To circumvent this difficulty, we instead compute the resummation

8

correction $\Delta\gamma_{NLO}^{+\,res}$ using a rational approximation to $\gamma_{NLO}^{+;\,cut}$ eq. (2.26), $\gamma_{NLO}^{+;\,rat}$, which is accurate when N is small (in the resummation region), and goes away at large N (where it is irrelevant), but is free of cuts. Thus we extend the double–leading expansion eq. (2.14) from $n_f = 0$ to $n_f \neq 0$ by adding to it $\gamma_{NLO}^{+;\,rat}$ instead of $\gamma_{NLO}^{+;\,cut}$, include the n_f dependent pieces in χ_1, and then follow from then onwards the same procedure as before as far as eqn.(2.22), to give us $\gamma_{NLO}^{+\,res,rat}(\alpha_s, N; n_f)$. Subtracting the $n_f = 0$ anomalous dimension then gives us the desired result:

$$\Delta\gamma_{NLO}^{+\,res}(\alpha_s, N; n_f) = \gamma_{NLO}^{+\,res,rat}(\alpha_s, N; n_f) - \gamma_{NLO}^{+\,res}(\alpha_s, N; 0), \qquad (2.27)$$

free from cuts. This procedure ensures that the resummed anomalous dimension is everywhere accurate, provided only the rational approximation is accurate in the small $N \lesssim 0.5$ region where the resummation kicks in: for larger values of N, where the resummed and unresummed results coincide by construction, and the exact γ_{NLO}^{+} is restored, complete with cut.

The rational approximation itself is constructed as a systematic improvement of the Laurent expansion of $\gamma_{NLO}^{+\,cut}$ eq. (2.26), about its leading singularity at $N = 0$. It is based on the physical requirements that it must only has singularities on the negative real axis, so the small x behaviour of the associated splitting function is only modified by terms suppressed by powers of x, and that it goes to a constant at large N, so that no large cancellations occur when the exact large N behaviour is restored. Finally, exact momentum conservation is imposed consistent with these requirements. In practice, we first construct a i–th order approximation

$$\bar{\gamma}_{(1)}^{rat}(N) = c_{-1}\frac{1}{N} + c_0 + c_1\frac{N}{1+N},$$

$$\bar{\gamma}_{(2)}^{rat}(N) = c_{-1}\frac{1}{N} + c_0 + c_1\frac{N(1+2N)}{(1+N)^2} + c_2\frac{N^2}{(1+N)^2},$$

$$\bar{\gamma}_{(3)}^{rat}(N) = c_{-1}\frac{1}{N} + c_0 + c_1\frac{N(1+3N+3N^2)}{(1+N)^3} + c_2\frac{N^2(1+3N)}{(1+N)^3} + c_3\frac{N^3}{(1+N)^3}, \quad \text{etc,}$$

$$(2.28)$$

where the polynomials in the numerator of the rational coefficients of c_i are adjusted so that

$$\bar{\gamma}_{(i)}^{rat}(N) = \sum_{k=-1}^{i} c_k N^k + O(N^{k+1}). \qquad (2.29)$$

We then impose momentum conservation while preserving eq. (2.29):

$$\gamma_{(i)}^{rat}(N) = \bar{\gamma}_{(i)}^{rat}(N) - \left(\frac{2N}{1+N}\right)\bar{\gamma}_{(i)}^{rat}(1). \qquad (2.30)$$

The rational approximations to $\gamma_0^+(N)$ eq. (2.13) is constructed by using eq. (2.30), with the first i coefficients c_i equated to the coefficients of the Laurent expansion of $\gamma_0^+(N)$ about $N = 0$. The same procedure can be used for $\gamma_1^+(N)$, and in fact also for the subsequent

orders $\gamma_k^+(N)$ by simply adding the necessary negative powers of N to reproduce higher order poles at $N = 0$.

Clearly, the rational approximation can be made arbitrarily accurate at small N by adding more terms; however the subsequent terms of the expansion, as the order of the approximation is increased, build up again the spurious cut singularity at N_d. In practice, we find that the quadratic approximation $\gamma_{rat}^2(N)$ is adequate: its accuracy is better than 1% at leading order for $N \leq 0.5$ and better than 8% for the next–to–leading order term, which in turn is however a few percent of $\gamma_{\rm NLO}^+$. For $N \leq 0.3$ these figures drop to 0.2% and 2% respectively. Since the n_f dependence of the resummation is itself only a small correction to the result when $n_f = 0$, this is sufficient for our purposes.

Equation (2.25) with the resummed anomalous dimension computed using the rational approximation $\gamma_{NLO,\,rat}^{+\,res}$ now gives us a resummed expression for the large eigenvalue of the anomalous dimension matrix. The NLO resummation is obtained by combining this with the standard NLO unresummed expression for the small eigenvalue γ^-. A full solution of the evolution equation is then obtained in terms of the two eigenvalues, and projectors $\mathcal{M}_\pm(\alpha_s, N)$ on the eigenvectors of the anomalous dimension matrix, such that

$$\gamma = \mathcal{M}_+\gamma^+ + \mathcal{M}_-\gamma^-\,, \qquad \mathcal{M}_+ + \mathcal{M}_- = \mathbb{1}\,, \quad \mathcal{M}_\pm\mathcal{M}_\pm = \mathcal{M}_\pm\,, \quad \mathcal{M}_\pm\mathcal{M}_\pm = 0. \quad (2.31)$$

The projectors eq. (2.31) have the form [12]

$$\begin{aligned}
\mathcal{M}_+ &= \frac{1}{\gamma^+ - \gamma^-}\begin{pmatrix} \gamma_{qq} - \gamma^- & \gamma_{qg} \\ X & \gamma^+ - \gamma_{qq} \end{pmatrix}\,, \\
\mathcal{M}_- &= \frac{1}{\gamma^+ - \gamma^-}\begin{pmatrix} \gamma^+ - \gamma_{qq} & -\gamma_{qg} \\ -X & \gamma_{qq} - \gamma^- \end{pmatrix}\,,
\end{aligned} \qquad (2.32)$$

where $X = (\gamma^+ - \gamma_{qq})(\gamma_{qq} - \gamma^-)/\gamma_{qg}$.

2.3. Resummed eigenvalues

In summary, we have completely specified the resummed form of the eigenvalues of the anomalous dimension. The small eigenvalue γ^- is not modified by the resummation and thus it is determined by fixed order perturbation theory. For the large eigenvalue the resummed result is obtained by combining eq. (2.22) with eqs. (2.25). All quantities appearing in these equations are either defined directly in this paper or in ref. [15]. From the expressions of the eigenvalues of the anomalous dimension we can construct the solutions of the evolution equations by using the projector formalism described above. The projectors $\mathcal{M}_\pm(\alpha_s, N)$ are fully determined from the knowledge of the eigenvectors $\gamma^\pm$ and the quark–sector matrix elements γ_{qq} and γ_{qg}.

The resummation of the quark sector anomalous dimensions requires understanding, at the resummed level, firstly how to combine coefficient functions with evolved parton distributions, and secondly how to select the factorization scheme. We will discuss both issues in the following two sections.

3. Resummation of physical observables

Resummed physical observables are obtained by combining parton distributions which obey resummed evolution equations with resummed coefficient functions. In the specific case of deep–inelastic scattering, we consider the flavour singlet component of the structure functions $F_2(x,t)$ and $F_L(x,t)$. Because, as already mentioned, in the nonsinglet channel the leading singularity at small x is suppressed by a power of x, we will not consider nonsinglet contributions and henceforth we will denote with F_i the singlet part of the structure functions. The N–Mellin transform of the structure functions

$$F_i(N,t) = \int_0^1 dx\, x^{N-1} F_i(x,t), \tag{3.1}$$

can generally be written in N space as

$$F_i(N,t) = c_q^i(N,\alpha_s(t))Q(N,t) + c_g^i(N,\alpha_s(t))G(N,t)$$
$$= c(N,\alpha_s(t))f(N,t), \tag{3.2}$$

where $f(N,t)$ is the parton distribution eq. (2.2),(2.3), and the elements $c_j^i(N,\alpha_s(t))$ ($i = 2,l$, $j = q,g$) of the matrix $c(N,\alpha_s(t))$ of coefficients are moments of a partonic cross section

$$c_j^i(N,\alpha_s(t)) = \int_0^1 dx\, x^{N-1}\, c_j^i(x,\alpha_s(t)). \tag{3.3}$$

3.1. Double leading expansion of the coefficient functions

In order to construct the small x expression of the coefficient functions we exploit the fact that the factorized expression eq. (3.2) can be derived from a more general k_T–factorization (or high–energy factorization) formula [21]. This factorization formula reduces to the more familiar k_T integrated form in the collinear limit, and is useful for our present purposes. The k_T–factorized form of structure functions is conveniently written in terms of the double Mellin transform eqs. (2.2),(2.8) of k^2–dependent coefficient functions $\mathcal{C}$ and parton distributions $\mathcal{F}$:

$$F_i(N,M) = \mathcal{C}_q^i(N,M,\hat{\alpha}_s)\mathcal{Q}(N,M;\mu^2) + \mathcal{C}_g^i(N,M,\hat{\alpha}_s)\mathcal{G}(N,M;\mu^2), \tag{3.4}$$

i.e., in vector notation:

$$F(N,M) = \mathcal{C}(N,M,\hat{\alpha}_s)\mathcal{F}(N,M;\mu^2). \tag{3.5}$$

The k^2–dependent coefficient functions are

$$\mathcal{C}_j^i(N,M) = \int \frac{dk^2}{k^2} \left(\frac{Q^2}{k^2}\right)^{-M} \sigma_j^i\left(\frac{Q^2}{k^2},N\right), \tag{3.6}$$

the Mellin transform of the partonic i-th structure function ($i = 2, L$) for scattering of a virtual photon with virtuality $-Q^2$ off a parton j ($j = q, g$) with virtuality $-k^2$.[2]

The coefficient function eq. (3.3) is obtained from eq. (3.4) using collinear factorization, i.e. extracting the collinear contribution to the Mellin inversion integral

$$F_i(N, t) = \int_{c-i\infty}^{c+i\infty} \frac{dM}{2\pi i} e^{Mt} F_i(N, M), \qquad (3.7)$$

where the integration path runs to the right of the singularities near $M = 0$ in the complex M plane. After factorizing all collinear logs in the evolution of the parton distribution, the coefficient function has a single collinear log, related to the integration over the transverse momentum of the corresponding off-shell parton line. Because upon M-Mellin transform powers of $t = \ln \frac{Q^2}{\mu^2}$ become powers of $\frac{1}{M}$, this means that the (M, N) space k_T–factorized parton distributions $\mathcal{F}(\mathcal{N}, \mathcal{M})$ have multiple $M = 0$ poles, whereas the coefficient functions $\mathcal{C}_j^i(N, M)$ have a simple pole. The contribution of these poles to the Mellin inversion integral eq. (3.7) then gives the collinear factorized result eq. (3.2), with

$$c_q^i(N, \alpha_s(t)) = C_j^i(N, M)\Big|_{M=0}, \qquad C_j^i(N, M) \equiv M\mathcal{C}_j^i(N, M), \qquad (3.10)$$

and

$$f(N, t) = \Gamma(N, t)f(N, 0), \qquad (3.11)$$

where $\Gamma(N, t)$ contains the contribution of the collinear M poles. The initial parton distribution, evaluated at $Q^2 = \mu^2$ (i.e. $t = 0$), is given by

$$f(N, 0) = \mathcal{F}(N, M; \mu^2)\Big|_{M=0}, \qquad (3.12)$$

as follows from an evaluation of the integral eq. (3.7) at $Q^2 = \mu^2$, where the parton distribution is free of poles.

The parton distribution satisfies the evolution equation (2.4) thanks to the t dependence due to the $M = 0$ poles included in the factor $\Gamma(N, t)$: specifically, eq. (2.6) for the large eigenvector (2.5) implies

$$\frac{d}{dt}\Gamma^+(N, t)f^+(N, \mu^2) = \int_{c-i\infty}^{c+i\infty} \frac{dM}{2\pi i} e^{Mt} M f^+(N, M)$$
$$= \gamma^+(\hat{\alpha}_s, N) \int_{c-i\infty}^{c+i\infty} \frac{dM}{2\pi i} e^{Mt} f^+(N, M). \qquad (3.13)$$

---

[2] The factorization formula of ref. [21] is yet more general, in that it applies to coefficient functions and parton distribution which depend on $\vec{k}$. Here we are not interested in the angular dependence and thus we discuss only the more restrictive version which is obtained from it after averaging over the angular dependence of $\vec{k}$ and only retaining the dependence on k^2.

It is useful to view this as an equation satisfied by $f^+(N, M)$ at the collinear pole [28]:

$$Mf^+(N, M) = \gamma^+(\hat{\alpha}_s, N)f^+(N, M). \tag{3.14}$$

The GLAP evolution equation (3.14) is, of course, satisfied to any logarithmic order thanks to the fact [33] that collinear singularities can be factored into the parton distribution. Hence, $\gamma^+(\hat{\alpha}_s, N)$ in eq. (3.14) is an operator which at the leading (next-to-leading, ...) $\ln Q^2$ level can be determined trivially from the GLAP kernel. Furthermore, using running–coupling duality [28], $\gamma^+(\hat{\alpha}_s, N)$ can also be determined at the leading (next-to-leading, ...) $\ln x$ level from the BFKL kernel.

High–energy factorization thus reproduces collinear factorization, in that the coefficient function thus obtained coincides with the collinear coefficient function eq. (3.8), while the parton distribution satisfies the GLAP equation (3.14).

However, here the main interest of k_T factorization is that at high energy eq. (3.4) holds even away from the collinear $M = 0$ pole, namely, the Mellin inverse eq. (3.7) of the k_T-factorized structure function eq. (3.4) gives the correct expression for the structure function, at least at the leading $\ln x$ level. This is sufficient for the determination [22] of the structure functions to the next-to-leading $\ln x$ level, and thus for the construction of the next-to-leading order of the double–leading expansion [12] of the coefficient functions, because the coefficients $\mathcal{C}_j^i(N, M)$ have the form

$$\mathcal{C}(N, M) = \frac{1}{M}\left[C_0 + \hat{\alpha}_s C_1(N, M) + O(\hat{\alpha}_s^2)\right], \tag{3.15}$$

with $C_0 = \begin{pmatrix} 1 & 0 \\ 0 & 0 \end{pmatrix}$.

The expansion of $c(N, \alpha_s(t))$ in powers of $\alpha_s(t)$ at fixed $\alpha_s(t)/N$ can then be determined to first nontrivial order (i.e. to next-to-leading $\ln x$ order) using eq. (3.14). Indeed, by dividing and multiplying by M the right–hand side of the factorized expression (3.5) and performing the Mellin inversion integral, we get

$$F(N, t) = C_0 f(N, t) + \alpha_s(t)\int_{c-i\infty}^{c+i\infty}\frac{dM}{2\pi i}e^{Mt}C_1(N, M)f(N, M) + O(\alpha_s^2(t)), \tag{3.16}$$

where $f(N, t)$ is the parton distribution eq. (3.11), $f(N, M)$ its Mellin transform (2.8), and C_0, C_1 are as in eq. (3.15).

However, the GLAP equation (2.6),(3.14) implies that, at the collinear pole, the integrals

$$I_k \equiv \int_{c-i\infty}^{c+i\infty}\frac{dM}{2\pi i}e^{Mt}M^k f(N, M) \tag{3.17}$$

are equal to:

$$\begin{aligned} I_1 &= \gamma(\alpha_s(t), N)f(N, t), \\ I_2 &= \left(\gamma^2 + \dot{\gamma}\right)f(N, t), \\ I_3 &= \left(\gamma^3 + 3\gamma\dot{\gamma} + \ddot{\gamma}\right)f(N, t), \qquad \text{etc.} \end{aligned} \tag{3.18}$$

13

The dot denotes differentiation with respect to t and γ is the anomalous dimension matrix acting on the parton distributions $f(N, t)$ eq. (3.11). Of course, all contributions proportional to t derivatives of γ on the right–hand side of eq. (3.18) vanish at the fixed coupling level. Note that eq. (3.16) only holds at the leading $\ln x$ level, but eqs. (3.17)-(3.18) follow from the GLAP equation and thus hold at all logarithmic orders.

If $\gamma(\alpha_s, N) = \gamma_s \left(\frac{\alpha_s}{N} \right)$ (leading $\ln x$), then $\dot{\gamma}$ is next-to-leading $\ln x$ and so forth: hence all terms beyond the first in round brackets on the r.h.s. of eq. (3.18) are subleading, so up to subleading terms $I_n = \gamma^n f$. Furthermore, $C(N, M)$ is regular as $N \to 0$ because all N–poles i.e. all logs of x are included in the evolution: we can thus set $N = 0$ in it, since positive powers of N lead to subleading contributions. It follows that the expansion of $c(N, \alpha_s(t))$ in powers of α_s at fixed α_s/N is

$$c(N, \alpha_s(t)) = C_0 + \alpha_s(t) c_{ss} \left(\gamma_s^+ \left(\frac{\alpha_s(t)}{N} \right) \right) \mathcal{M}_+ + O(\alpha_s^2) \qquad (3.19)$$

where $\mathcal{M}_+$ is the projector eq. (2.31), and

$$c_{ss}(M) = C_1(0, M). \qquad (3.20)$$

In order to derive eq. (3.19) we inserted $\mathbb{1} = \mathcal{M}_+ + \mathcal{M}_-$ in eq. (3.16) between C_1 and f and recalled that $\gamma_s^- = 0$ (see eq. (2.5)). The explicit expression for the four matrix elements $c_{ss}(M)$ in the $\overline{\mathrm{MS}}$ scheme is given in ref. [22].

The double leading expression for the coefficient function is obtained combining the first k orders of the expansion of $c(N, \alpha_s(t))$ in powers of α_s at fixed α_s/N with the first k orders of the standard expansion of $c(N, \alpha_s(t))$ in powers of α_s at fixed N, and subtracting double counting: up to next-to-leading order

$$c_{\mathrm{DL}}(N, \alpha_s(t)) = C_0 + \alpha_s(t) \left[(c_1(N) - c_1(0)) + c_{ss} \left(\gamma_{\mathrm{NLO}}^{+\,res} (\alpha_s(t), N) \right) \mathcal{M}_+ \right] + \cdots, \quad (3.21)$$

where $c_1(0)$ is the subtraction for double counting, and $\gamma_{\mathrm{NLO}}^{+\,res}$ is the resummed anomalous dimension eq. (2.25). The identification of the second argument of c_{ss} with $\gamma_{\mathrm{NLO}}^{+\,res}$ follows from eq. (3.18) with $\gamma = \gamma_{\mathrm{NLO}}^{+\,res}$, neglecting all subleading terms with t derivatives of γ. Of course, the replacement of the leading $\ln x$ expression γ_s^+ with $\gamma_{\mathrm{NLO}}^{+\,res}$ is also subleading. Nevertheless, this replacement is needed in order to ensure that the coefficient function in N space doesn't develop a spurious singularity at the location of the cut in γ_s^+, which, being to the right of the singularity (simple pole) which dominates the small x behaviour of $\gamma_{\mathrm{NLO}}^{+\,res}$ (see fig. 6 of ref. [15]), would lead to large, spurious small x corrections.

3.2. Running coupling effects

We have seen in Sect. 2 that running coupling corrections to the anomalous dimension start at next-to-leading $\ln x$ (2.18), but their all–order resummation is necessary to obtain a stable small x limit, because their leading singularities are of increasingly higher order at higher orders in $\beta_0 \alpha_s$. The all–order resummation of these singular terms actually changes the nature of the leading singularity which dominates the small x behaviour of the anomalous dimension and associated splitting function.

Running coupling corrections to the coefficient functions, namely the terms proportional to t derivatives of the anomalous dimension in eq. (3.18), start at next-to-next-to-leading $\ln x$. It is easy to see that they also have leading singularities of increasingly high order. Indeed, differentiating the duality relation (2.10) with respect to t we get

$$\dot{\gamma}^+(\alpha_s, N) = -\left.\frac{\dot{\chi}(\alpha_s, M)}{\chi'(\alpha_s, M)}\right|_{M=\gamma(\alpha_s, N)}, \tag{3.22}$$

where the dot denotes differentiation with respect to t and the prime indicates differentiation with respect to M. This expression is clearly singular at the minimum of χ: indeed, after running–coupling resummation of the anomalous dimension, γ has a simple pole at $N_0(\alpha_s(t))$ eq. (2.20). Hence, subsequent t derivatives of γ will have higher order poles there. It follows that the double–leading result eq. (3.21) is not stable at small x: the running–coupling corrections to the coefficient function must also be resummed to all orders. This can be done using the technique developed in ref. [24], and (as in the case of the anomalous dimension) it changes the nature if the singularity which dominates the small x behaviour of the coefficient function.

After factorization of the collinear $M = 0$ poles, the coefficient functions $c_{ss}(M)$ have simple poles on the real M axis for positive and negative values of M [22]. Those for negative values of M correspond to higher-twist corrections and are of no concern. Those for positive values of M start at $M = 1$, i.e. at the edge of the physical region for the Mellin inversion integral eq. (2.8) and thus also seem immaterial. Nevertheless, if we let $M = \gamma^{+\,res}_{\rm NLO}$ as in eq. (3.21), then at small x the resummed anomalous dimension is dominated by the pole eq. (2.20), so, using the form eq. (2.20) of $\gamma(\alpha_s, N)$, a simple pole in the coefficient function at $M = k$ becomes

$$\left.\frac{1}{k - M}\right|_{M=\gamma(\alpha_s, N)} = \frac{(N - N_0)/k}{N - (N_0 + r/k)}, \tag{3.23}$$

which has a pole to the right of the pole of the anomalous dimension. The pole in the coefficient function at $M = 1$, after running coupling resummation of the anomalous dimension but in the absence of running coupling resummation of the coefficient function, would thus become the leading small x singularity. This is due to the fact that the identification $M = \gamma^+(\alpha_s, N)$ in the coefficient function is equivalent to dominating the Mellin inversion integral eq. (3.16) with a simple pole at $M = \gamma^+(\alpha_s, N)$, but if γ^+ has the form eq. (2.20), as N decreases this pole actually moves to the right of $M = 1$ thereby pinching the path of M integration. Note that at the fixed coupling level this does not happen because the anomalous dimension at small x then has the form eq. (2.17), which is bounded by M_0 and thus does not lead to any new singularities.

However, the singularity eq. (3.23) is entirely spurious: indeed, it can be shown [24] that the Mellin inversion integral for a coefficient function which has a simple pole in M and a parton distribution which satisfies the running–coupling GLAP equation (3.13) has no new N singularities on top of those already present in the parton distributions. In particular, we can explicitly check this statement by performing the integral in the case of a coefficient function given by a simple pole and an anomalous dimension linear in α_s.

15

In fact, taking $\gamma^+ = \alpha_s(t)\gamma_0^+$, and using the leading order β function $\beta(\alpha_s) = -\beta_0\alpha_s^2$, the integral for any parton density f can be computed exactly [24]:

$$J(N,t) \equiv \int_{c-i\infty}^{c+i\infty} \frac{dM}{2\pi i} e^{Mt} \frac{1}{1-M} f(N,M) = t^{-\gamma_0(N)/\beta_0} e^t \Gamma(1+\gamma_0(N)/\beta_0, t) f(N,t), \quad (3.24)$$

where $\Gamma(x,t)$ is the incomplete Gamma function. Manifestly, $J(N,t)$ eq. (3.24) is free of N singularities besides those already present in $f(N,t)$. In this case, it can further be shown explicitly that the series of running coupling contributions on the right–hand side of eq. (3.18) is an asymptotic expansion of the exact singularity–free result. Indeed, in this case higher order t derivatives of γ can all be expressed in terms of $\dot\gamma$ and γ, and eq. (3.18) becomes

$$I_k = [\gamma^k] f(N,t), \quad (3.25)$$

where we have defined $[\gamma^k]$ as follows:

$$[\gamma] = \gamma(\alpha_s(t), N),$$
$$[\gamma^2] = \gamma^2 \left(1 + \frac{\dot\gamma}{\gamma^2}\right), \quad (3.26)$$
$$[\gamma^3] = \gamma^3 \left(1 + \frac{\dot\gamma}{\gamma^2}\right)\left(1 + 2\frac{\dot\gamma}{\gamma^2}\right), \quad \text{etc},$$

so that recursively

$$[\gamma^n] = \gamma \left(1 + (n-1)\frac{\dot\gamma}{\gamma^2}\right)[\gamma^{n-1}]. \quad (3.27)$$

It is then easy to see that if we determine $J(N,t)$ eq. (3.24) by integrating the series expansion of $\frac{1}{1-M}$ term by term

$$J(N,t) = \sum_{k=0}^{\infty} [\gamma^k] f(N,t) \quad (3.28)$$

and use eq. (3.26) we recover eq. (3.24) with the standard asymptotic expansion of $\Gamma(x,t)$ in inverse powers of t.

In summary the all-order resummation of the increasingly more divergent running coupling corrections eq. (3.18) removes the spurious singularity eq. (3.23) which is produced if these running coupling terms are neglected but the running coupling resummation is included in the anomalous dimension. We could thus proceed analogously to the running coupling resummation of the anomalous dimension: subtract the M poles from the coefficient function, resum them using the exact result of ref. [24], and treat the remaining regular part of the coefficient function in the $M = \gamma$ approximation, the corrections to which are now genuinely subleading. However, in the $\overline{\text{MS}}$ scheme, only the F_L coefficient functions, i.e. the second column of the matrix $c_1(M)$ are known in closed form, whereas for the F_2 coefficient functions only a series expansion in powers of M is known [22], and this procedure is not viable.

16

However, we may instead use the explicit result eq. (3.26) to perform the inverse Mellin transform order by order using the power series expansion of the coefficient function. Indeed, eq. (3.26) was derived assuming the leading order form of γ and the running of α_s. Hence, for a generic anomalous dimension $\gamma(N, t)$ it holds up to $O(\alpha_s^2)$ corrections. Furthermore, we know that, for a coefficient function which has simple poles, if running coupling terms are included to all orders in α_s (in the expanded case using eq. (3.18)) the coefficient function does not have any singularities. Because the result to $O(\alpha_s)$ found using eq. (3.26) is already free of singularities, it follows that the remaining corrections are genuinely subleading. We conclude that a running coupling resummation of c_{DL} eq. (3.21) is given by

$$
\begin{aligned}
c_{\mathrm{DL}}(N, \alpha_s(t)) = C_0 + \alpha_s(t) \Big\{ (c_1(N) - c_1(0)) + \Big[c_{ss} \left([\gamma_{\mathrm{NLO}}^{+\,res}] \right) \\
- c_{ss}([\gamma_0^+(N) + \alpha_s \gamma_1^+(N) - \tfrac{\alpha_s}{N} \left(\tfrac{n_c}{\pi} - \alpha_s e_1^+ \right) - e_2^+ \tfrac{\alpha_s^2}{N^2}]) \Big] \mathcal{M}_+ \Big\},
\end{aligned}
$$

$$(3.29)$$

where by $c_{ss}([\gamma_{\mathrm{NLO}}^{+\,res}])$ we mean that $c_{ss}(M)$ is expanded in powers of M, and then evaluated by replacing M^k with $[\gamma^k]$ and using eq. (3.26) with $\gamma = \gamma_{\mathrm{NLO}}^{+\,res}$. The term on the last line is a matching term: it has been chosen to ensure that at large N, where $\gamma_{\mathrm{NLO}}^{+\,res}$ reduces to $\gamma_0^+(N) + \alpha_s \gamma_1^+(N)$, the coefficient reduces to its standard large N form, while at small N it reduces to $c_{ss}([\gamma_{\mathrm{NLO}}^{+\,res}])$, as it should.

In practice, use of eq. (3.29) is subject to the limitation that the series expansion that one obtains is only asymptotic, and it must thus be truncated after a finite number of terms. Clearly, the divergence sets in earlier at small Q^2 and small x, where the anomalous dimension $\gamma(N, \alpha_s)$ grows large, Unfortunately, it turns out that for typical values of the kinematic variables, such as $x \lesssim 10^{-3}$, $\alpha_s \gtrsim 0.2$, the series for the matrix elements already starts diverging after a rather small number of terms, which leads to an unacceptably large ambiguity in the results.

However, we can treat the asymptotic series by Borel resummation. Namely, the n-th order contribution to eq. (3.26) is written as

$$
[\gamma^n] = \int_0^\infty ds\, K(s) \frac{s^n}{f(n)} \gamma^n \left(1 + \frac{\dot{\gamma}}{\gamma^2} \right) \dots \left(1 + (n-1)\frac{\dot{\gamma}}{\gamma^2} \right),
$$

$$(3.30)$$

where $K(s)$ is chosen in such a way that $f(n)$ grows with n, thereby improving the convergence of the series. For instance, the standard choice is

$$
K(s) = e^{-s}, \quad f(n) = n!.
$$

$$(3.31)$$

With this choice, in the specific case of $J(N, t)$ eq. (3.24) the divergent series eq. (3.24) becomes convergent, and one gets

$$
J(N, t) = c(N, t) f(N, t),
$$

$$(3.32)$$

$$
c(N, t) = \int_0^\infty ds\, e^{-s} c(N, t; s),
$$

$$(3.33)$$

$$
c(N, t; s) = \left[1 - s \frac{\dot{\gamma}(N, \alpha_s(t))}{\gamma(N, \alpha_s(t))} \right]^{-\gamma^2/\dot{\gamma}}.
$$

$$(3.34)$$

However, the expansion of $c(N, t; s)$ eq. (3.32) in powers of s has finite radius of convergence. Because in general we cannot sum the series in closed form, this would prevent a numerical evaluation of the integral over s eq. (3.30). We can solve this problem by choosing $K(s)$ in such a way that $f(n)$ grows more than factorially with n. Specifically, we make the choice

$$K(s) = K_0(\sqrt{s}); \quad f(n) = (n!)^2, \tag{3.35}$$

where K_0 is a modified Bessel function. Now

$$c(N, t) = \int_0^\infty ds \, K_0(\sqrt{s}) \bar{c}(N, t; s), \tag{3.36}$$

and the expansion of $\bar{c}(N, t; s)$ has infinite radius of convergence, because its n–th order term is factorially smaller than the corresponding term in the series expansion of $c(N, t; s)$ which had finite radius of convergence. In the particular case of $J(N, t)$ eq. (3.24), the function $\bar{c}(N, t; s)$ eq. (3.36) is given by

$$\bar{c}(N, t; s) = M\left(\tfrac{\gamma^2}{\dot\gamma}, 1, s\tfrac{\dot\gamma}{\gamma}\right), \tag{3.37}$$

where $M(x, y, z)$ is the confluent hypergeometric function.

We can thus use eq. (3.36) to evaluate the series expansion of the coefficient function eq. (3.29), at least to the extent that the dominant singularities of the coefficient function are poles. In practice, since we only know the expansion of c_{ss} in powers of M, we cannot sum the power series expansion in closed form before performing the Borel inversion integral over s eq. (3.32). This seems problematic because the integral of any finite–order truncation of the expansion of the right–hand side of eq. (3.32) leads back to the original divergent series. Nevertheless, if the Borel inversion integral exists, then one can obtain an arbitrarily accurate approximation to it by integrating up to a given cutoff Λ. But because the series has infinite radius of convergence, for any finite value of Λ the integrand can be determined to any desired accuracy by including a finite number of terms in the series. In practice, instead of truncating the s integration at some large cutoff value, we may replace $\bar{c}(N, t; s)$ with an extrapolation for $s > \Lambda$, either linear, or based on the hypergeometric form eq. (3.37).

3.3. Resummed coefficient functions

Summarizing, we constructed a resummed coefficient function based on the running–coupling resummation of the double leading coefficient function eq. (3.21). The result has the form eq. (3.29), where the running coupling resummation is effected by evaluating the argument of the next-to-leading $\ln x$ coefficient functions c_{ss} by means of eq. (3.26). The ensuing divergent series are summed through Borel transformation eq. (3.36). The Borel transformed series is truncated and summed numerically, and the Borel inversion integral is also performed numerically by integrating up to a cutoff Λ, whence it is extrapolated using the form of eq. (3.37), which gives the contribution to the series from the dominant $M = 1$ pole. The accuracy of the result can is verified by checking its approximate independence of the chosen value of the cutoff Λ.

18

4. Factorization schemes and the quark sector

A factorization scheme change is a redefinition of the parton distribution of the form

$$f'(N, t) = U(N, \alpha_s(t)) f(N, t). \tag{4.1}$$

Invariance of physical observables them implies that coefficient functions transform as

$$C'(N, t) = C(N, t) U^{-1}(N, \alpha_s(t)). \tag{4.2}$$

The anomalous dimensions in the primed and unprimed schemes eq. (4.1) are then related by

$$\gamma'(N, \alpha_s(t)) = U(N, \alpha_s(t)) \gamma(N, \alpha_s(t)) U^{-1}(N, \alpha_s(t)) + \frac{d}{dt} U(N, \alpha_s(t)) U^{-1}(N, \alpha_s(t)). \tag{4.3}$$

4.1. Resummed factorization schemes

The theory of factorization scheme changes at the resummed level has been developed in ref. [25], and in ref. [12] at the double leading level; we recall some of the main results. If we consider the effect of a change of factorization scheme both on the expansion of anomalous dimension in powers of α_s at fixed N eq. (2.13) and at fixed α_s/N eq. (2.11), the requirement that a change in factorization scheme leaves the leading–order anomalous dimension invariant allows a wider class of factorization scheme changes at small x. This is a consequence of the fact that the leading $\ln x$ anomalous dimension matrix has the form

$$\gamma_s = \begin{pmatrix} 0 & 0 \\ \gamma_s^{gq}\left(\frac{\alpha_s}{N}\right) & \gamma_s^{gg}\left(\frac{\alpha_s}{N}\right) \end{pmatrix}, \tag{4.4}$$

where the nonvanishing entries satisfy the colour-charge relation

$$\gamma_s^{gq} = \frac{C_F}{C_A} \gamma_s^{gg}. \tag{4.5}$$

It follows that if parton distributions are redefined by a leading $\ln x$ function $U_s(\frac{\alpha_s}{N})$, the leading $\ln x$ anomalous dimension eq. (4.4) is unchanged provided only [25]

$$U_s\left(\frac{\alpha_s}{N}\right) = \begin{pmatrix} 1 & 0 \\ \frac{C_F}{C_A} z_s^{gg}\left(\frac{\alpha_s}{N}\right) & z_s^{gg}\left(\frac{\alpha_s}{N}\right) \end{pmatrix}, \tag{4.6}$$

where $z_s^{gg}(\frac{\alpha_s}{N}) = 1 + z_{s,1}^{gg} \frac{\alpha_s}{N} + \dots$.

The scheme change eq. (4.6) is thus a redefinition of the small x normalization of the gluon distribution, and it changes γ^{qg} and γ^+ according to

$$\begin{aligned} \gamma_{ss}^{qg\,\prime} &= \gamma_{ss}^{qg}/u(\gamma_s^+) \\ \gamma_{ss}^{+\,\prime} &= \gamma_{ss}^+ + \frac{\beta_0}{4\pi} \frac{\chi_0(\gamma_s^+)}{\chi_0'(\gamma_s^+)} \frac{d \ln u}{dM}\bigg|_{M=\gamma_s^+}, \end{aligned} \tag{4.7}$$

19

where the function $u(M)$ is defined by the implicit equation

$$z_s^{gg}(\tfrac{\alpha_s}{N}) = u(\gamma_s(\tfrac{\alpha_s}{N})). \tag{4.8}$$

Further small x scheme changes have the standard next-to-leading form

$$U(N, \alpha_s) = \mathbb{1} + \alpha_s z_{ss}\left(\tfrac{\alpha_s}{N}\right), \tag{4.9}$$

where $z_{ss}(0) = 0$. The scheme change eq. (4.9) affects the next-to-leading $\ln x$ anomalous dimension according to

$$\gamma'_{ss} = \gamma_{ss} + [z_{ss}, \gamma_s]. \tag{4.10}$$

The form eq. (4.4),(4.5) of γ_s implies that the effect on the anomalous dimensions of a scheme change of the form of eq. (4.9) is particularly simple [25]:

$$\gamma' = \gamma + \begin{pmatrix} \frac{C_F}{C_A} z_{ss}^{qg}\left(\tfrac{\alpha_s}{N}\right) & z_{ss}^{qg}\left(\tfrac{\alpha_s}{N}\right) \\ \frac{C_F}{C_A}\left(z_{ss}^{gq}\left(\tfrac{\alpha_s}{N}\right) - z_{ss}^{qg}\left(\tfrac{\alpha_s}{N}\right)\right) - z_{ss}^{gg}\left(\tfrac{\alpha_s}{N}\right) & \frac{C_F}{C_A} z_{ss}^{qg}\left(\tfrac{\alpha_s}{N}\right) \end{pmatrix} \gamma_s^{gg}. \tag{4.11}$$

This is useful since the component γ_{gq} of γ_{ss} in fact has no effect on a calculation at the next-to-leading order of the resummed or double–leading expansion [12], so in practice at NLO it is only necessary to fix z_{ss}^{qg}.

It is interesting to observe that the form eq. (4.4),(4.5) of γ_s, together with the requirement eq. (2.5) that only one of the two eigenvalues of γ has leading small x singularities, also entails some scheme–independent relations between singular contributions to matrix elements of γ. Indeed, the trace and determinant conditions for the eigenvalues $\gamma^\pm$, if the singular contributions to γ^- vanish, imply

$$\gamma^{gg} + \gamma^{qq} = \gamma^+; \quad \gamma^{gg}\gamma^{qq} = \gamma^{qg}\gamma^{gq}. \tag{4.12}$$

These relations clarify the meaning of the colour-charge relation. Indeed, to next-to-leading $\ln x$ the second of eq. (4.12), when combined with eq.(4.5), implies that

$$\gamma_{ss}^{qq}(\tfrac{\alpha_s}{N}) = \tfrac{C_F}{C_A}(\gamma_{ss}^{qg}(\tfrac{\alpha_s}{N}) - \gamma_{ss}^{qg}(0)). \tag{4.13}$$

To higher orders, the colour charge relation is sufficient but not necessary for eq. (4.12) to hold.

4.2. Construction of the $\overline{\mathrm{MS}}$ and $Q_0\overline{\mathrm{MS}}$ schemes.

Let us now turn to the explicit construction of factorizations schemes, in order to construct resummed physical observables. To this purpose, we first summarize the available information on the coefficient functions and quark–sector anomalous dimensions in various factorization schemes. The leading small x coefficient function matrix (i.e. the function $c_{ss}(M)$ eq. (3.20)), as well as the anomalous dimension γ_{qg} (and thus γ_{qq}, by eq. (4.13)) have been determined at leading order in ref. [22] in both the $\overline{\mathrm{MS}}$ and DIS schemes. In particular, γ_{qg} takes the form

$$\gamma_{ss}^{qg}(\tfrac{\alpha_s}{N}) = h\left(\gamma^+(\tfrac{\alpha_s}{N})\right), \tag{4.14}$$

where the function $h(M)$ may be extracted from the computation of the quark–antiquark production cross section from photon–virtual gluon fusion, using the high–energy factorization techniques discussed in sect. 3.2. In the DIS scheme the function $h(M)$ is known in closed form, while in $\overline{\text{MS}}$ $h(M)$ and $c_{ss}(M)$ are known to all orders in their power series expansion about $M = 0$.

The DIS scheme is defined by the identification of the structure function F_2 with the quark distribution: $F_2(x, Q^2) = Q^{\text{DIS}}(x, t)$. This does not fix the scheme completely, but it is sufficient to fix it at the next-to-leading $\ln x$ level. In particular, because $C_g^{2,\,\text{DIS}} = 0$, eq. (4.2) immediately implies that for the DIS$\rightarrow\overline{\text{MS}}$ scheme change

$$
\begin{aligned}
z^{qq}(N, \alpha_s(t)) &= 1 - C_q^{2,\,\overline{\text{MS}}}(N, \alpha_s(t)) \\
z^{qg}(N, \alpha_s(t)) &= -C_g^{2,\,\overline{\text{MS}}}(N, \alpha_s(t)).
\end{aligned}
\tag{4.15}
$$

Due to eq. (4.11) and the fact that γ_{gq} is only relevant at the next-to-next-to leading $\ln x$ level, the effect of the scheme change is thus fully determined.

The small x singular contributions to the large eigenvalue γ^+ eq. (2.11) are the same in the $\overline{\text{MS}}$ and DIS schemes: indeed, eq. (4.10) implies that up to this order the trace $\text{Tr}\gamma = \gamma^+ + \gamma^-$ is invariant, but the singular part of γ^- vanishes in both schemes, so γ^+ is invariant. Hence γ_{ss}^+ in eq. (2.14) is the same in the DIS and $\overline{\text{MS}}$ scheme.

The function γ_{ss}^+ on which the resummation of ref. [15] is based, as summarized in sect. 2, is however given in a scheme which differs from $\overline{\text{MS}}$ by a small-x scheme change eq. (4.11), the so–called $Q_0\overline{\text{MS}}$ scheme [34]. This is due to the fact that in the $\overline{\text{MS}}$ scheme the running coupling corrections to duality eq. (2.18), order by order in the expansion eq. (2.11) in powers of α_s at fixed α_s/N, are actually factorized in the coefficient function. These schemes are thus not suitable for the resummation eq. (2.19) of the running coupling corrections, because the singular contributions whose all–order resummation determines the leading small x singularity sits in the coefficient function. The scheme–change function $u(M)$ which takes us from the $\overline{\text{MS}}$ scheme to the $Q_0\overline{\text{MS}}$ scheme is of the form [15,21,8]

$$
u(M) = \frac{r(M)}{\sqrt{-\chi_0'(M)}},
\tag{4.16}
$$

where χ_0 is the leading-order BFKL kernel eq. (2.9) and the function $r(M)$ is regular in $0 < \text{Re}M < 1$. Using eq. (4.16) in eq. (4.7) one sees explicitly that the singular running–coupling contribution eq. (2.18) is removed from the $Q_0\overline{\text{MS}}$ scheme anomalous dimension γ_{ss} and factored in the coefficient function when transforming to the $\overline{\text{MS}}$ scheme.

Clearly, in a consistent calculation the coefficient functions and the anomalous dimensions must all be computed in the same scheme. Here we have (at least) two choices: either we can work in the $Q_0\overline{\text{MS}}$ scheme throughout, or we can work in the $\overline{\text{MS}}$ scheme. If we choose to work in the $Q_0\overline{\text{MS}}$ scheme, using the $Q_0\overline{\text{MS}}$ scheme resummed anomalous dimension γ^+ eq. (2.25), we must transform the coefficient functions and quark–sector anomalous dimensions of ref. [22] from the $\overline{\text{MS}}$ scheme by means of the scheme change function eq. (4.16). Alternatively, if we choose to work in the $\overline{\text{MS}}$ (or DIS) scheme, we take the coefficient functions and quark sector anomalous dimensions from ref. [22], then we

perform the resummation of γ^+ in the $Q_0\overline{\text{MS}}$ scheme as discussed in sect. 2.3, and finally we transform γ^+ from $Q_0\overline{\text{MS}}$ scheme to $\overline{\text{MS}}$ using (4.16) and (4.7). Because it is performed after the resummation of γ^+, the scheme change results in subleading terms which multiply the resummed parton distribution, in the same way as a coefficient function, its singularities, and in particular the singularity at $M = \frac{1}{2}$, eq. (4.16), may be treated in the same way as the pole in eq. (3.24), i.e. removed by running coupling resummation.

Let us discuss these two alternatives in detail. When working in $Q_0\overline{\text{MS}}$ scheme, we start from $\gamma_{ss}^{qg,\overline{\text{MS}}}(\frac{\alpha_s}{N})$ and $c_1^{\overline{\text{MS}}}(N, M)$. We then define [30] the Q_0 version of the $\overline{\text{MS}}$ scheme by constructing a scheme change based on the requirements that γ^+ be as in the $Q_0\overline{\text{MS}}$ scheme, while γ_{ss}^{qg} is unchanged, i.e. the same as in the $\overline{\text{MS}}$ scheme. Assuming we perform the scheme change through a leading $\ln x$ scheme change eq. (4.11),(4.8), followed by a next-to-leading scheme change eq. (4.9), the first requirement fixes

$$z_s^{gg}\left(\tfrac{\alpha_s}{N}\right) = u\left(\gamma_s\left(\tfrac{\alpha_s}{N}\right)\right), \tag{4.17}$$

with $u(M)$ given by eq. (4.16), and the second requirement then, combining eq. (4.7) with eq. (4.11) and demanding invariance of γ_{ss}^{qg}, gives

$$z_{ss}^{qg}\left(\tfrac{\alpha_s}{N}\right) = \left(1 - \frac{1}{z_s^{gg}\left(\tfrac{\alpha_s}{N}\right)}\right)\frac{\gamma_{ss}^{qg,\overline{\text{MS}}}(\tfrac{\alpha_s}{N})}{\gamma_s^{gg}(\tfrac{\alpha_s}{N})} \equiv v\left(\gamma_s\left(\tfrac{\alpha_s}{N}\right)\right), \tag{4.18}$$

where

$$v(M) = \left(1 - \frac{1}{u(M)}\right)\frac{h(M)}{M}, \tag{4.19}$$

with $h(M)$ defined in eq. (4.14). Note that $v(M)$ is regular at $M = 0$ since $u(0) = 1$. Consequently, given the series expansion for the coefficient functions $c_{ss}(M)$ (eq. (3.20)) in $\overline{\text{MS}}$, we can turn them into series expansions for the coefficient functions in $Q_0\overline{\text{MS}}$ by means of the combined scheme change eqs. (4.17),(4.18): the result is

$$c_{ss}^{2,g\,Q_0}(M) = \frac{c_{ss}^{2,g\,\overline{\text{MS}}}(M)}{u(M)} - \left(1 + \frac{h(M)}{M}\right)\left(1 - \frac{1}{u(M)}\right),$$
$$c_{ss}^{L,g\,Q_0}(M) = \frac{c_{ss}^{L,g\,\overline{\text{MS}}}(M)}{u(M)}. \tag{4.20}$$

The quark coefficient functions are then given by the color-charge relation: modulo double counting terms,

$$c_{ss}^{2,q\,Q_0} = \frac{C_F}{C_A}c_{ss}^{2,g\,Q_0}; \quad c_{ss}^{L,q\,Q_0} = \frac{C_F}{C_A}c_{ss}^{L,g\,Q_0}. \tag{4.21}$$

Constructing the $\overline{\text{MS}}$ scheme is simpler in some respects, since the only scheme transformation necessary is that required to change γ^+ from $Q_0\overline{\text{MS}}$ to $\overline{\text{MS}}$, and this is given by (4.7),(4.8), and (the inverse of) (4.16). The main complication here is in the consistent treatment of running coupling effects, which is necessary because $u(M)$ is singular. The effect of this singularity arises when M acts on the parton distributions according

22

to eq. (3.18), so we can treat it with a prescription based on that which we used for the coefficient function in eq. (3.26):

$$\frac{d}{dt}[\gamma] = \dot{\gamma},$$

$$\frac{d}{dt}[\gamma^2] = 2\gamma\dot{\gamma}\left(1 + \frac{\dot{\gamma}}{\gamma^2}\right),$$

$$\frac{d}{dt}[\gamma^3] = 3\gamma^2\dot{\gamma}\left(1 + \frac{\dot{\gamma}}{\gamma^2}\right)\left(1 + 2\frac{\dot{\gamma}}{\gamma^2}\right), \qquad \text{etc.}$$

(4.22)

so that

$$\gamma^{+,\overline{\text{MS}}} = \gamma^+ - \frac{d}{dt}\ln u\left([\gamma_{\text{NLO}}^{+res}(\alpha_s(t), N)]\right),$$

$$+ \frac{d}{dt}\ln u\left([\gamma_0^+(N) + \alpha_s\gamma_1^+(N) - \frac{\alpha_s}{N}\left(\frac{n_c}{\pi} - \alpha_s e_1^+\right) - e_2^+ \frac{\alpha_s^2}{N^2}]\right),$$

(4.23)

where the second term is evaluated in practice by first expanding $u(\gamma)$ in powers of γ and then using (4.22). The last term is a matching term, chosen in just the same way as in eq. (3.29) to ensure that the resummation does not corrupt the anomalous dimension at large N (and thus the splitting function at large x).

4.3. Resummed quark anomalous dimensions

Once the scheme is fixed, we can construct all the resummed anomalous dimensions and coefficient functions. The anomalous dimension γ^+ and its resummation in $Q_0\overline{\text{MS}}$ scheme are as in ref. [15], as summarized in sect. 2 of the present paper. If we are working in $\overline{\text{MS}}$, we must also add to this the contribution eq. (4.23), as explained above.

The resummed quark sector anomalous dimensions are then built as follows. First, we note that γ^{qq} can be obtained from γ^{qg} using the colour–charge relation eq. (4.13). Furthermore, γ^{gg} and γ^{gq} can be obtained from γ^+ and the quark-sector entries of γ using eq. (4.12). Hence we concentrate on the construction of γ^{qg}. We start from $\gamma_{ss}^{qg,\overline{\text{MS}}}(\frac{\alpha_s}{N})$, written as in eq. (4.14). We then construct the double–leading expression

$$\gamma_{\text{DL}}^{qg}(\tfrac{\alpha_s}{N}) = \gamma_0^{qg}(N) + \alpha_s\gamma_1^{qg,\overline{\text{MS}}}(N) + \alpha_s\left(h\left(\gamma_s^{gg}(\tfrac{\alpha_s}{N})\right) - h(0) - h'(0)\tfrac{n_c}{\pi}\tfrac{\alpha_s}{N}\right), \qquad (4.24)$$

where the last two terms subtract the double counting. We then note that the function $h(M)$ eq. (4.14) has singularities in M analogous to those of the contribution from $c_{ss}(M)$ eq. (3.20) to the coefficient function: we treat these by running coupling resummation eq. (3.26). Putting everything together at the resummed level we thus get

$$\gamma_{\text{res}}^{qg}(\tfrac{\alpha_s}{N}) = \gamma_0^{qg}(N) + \alpha_s\gamma_1^{qg,\overline{\text{MS}}}(N) + \alpha_s h\left([\gamma_{\text{NLO}}^{+res}(\alpha_s(t), N)]\right)$$

$$- \alpha_s h\left([\gamma_0^+(N) + \alpha_s\gamma_1^+(N) - \tfrac{\alpha_s}{N}\left(\tfrac{n_c}{\pi} - \alpha_s e_1^+\right) - e_2^+ \tfrac{\alpha_s^2}{N^2}]\right)$$

$$- h(0)\alpha_s - h'(0)\left(\tfrac{n_c}{\pi} - \alpha_s e_1^+\right)\tfrac{\alpha_s}{N},$$

(4.25)

where by $h([\gamma])$ we mean that $h(M)$ is expanded in power series of M, and then evaluated using eq. (3.26). The terms in the last two lines are matching and double–counting terms, which have been constructed just as they were for the coefficient functions eq. (3.29).

This construction then gives us the resummed γ^{qg} both in the $\overline{\text{MS}}$ and $\text{Q}_0\overline{\text{MS}}$ scheme. The resummed coefficient functions in either the $\overline{\text{MS}}$ are then found using eq. (3.29) with the expression of c_{ss} given in ref. [22], while its counterpart in the $\text{Q}_0\overline{\text{MS}}$ scheme is found in the same way, but with c_{ss} given by the scheme change eqs. (4.20), evaluated as function of $[\gamma_{\text{NLO}}^{+\,res}]$ in the sense of eq. (3.26).

5. Phenomenological Implications

5.1. Splitting functions and coefficient functions

We now discuss the application of our results and their phenomenological impact. We start by presenting the $n_f \neq 0$ full matrix of resummed singlet splitting functions together with the coefficients c_q^i and c_g^i (i=2,L) for the singlet structure functions F_2 and F_L, respectively. The curves for the splitting functions for $\alpha_s = 0.2$, $n_f = 4$ (the average values relevant for HERA) versus $1/x$ are shown in figs. 1-2. There we show the plots of the gluon splitting functions xP_{gg} and xP_{gq} (fig. 1), and the quark splitting functions xP_{qq} and xP_{qg} (fig. 2) both in fixed order perturbation theory (at the LO, NLO and NNLO level) and in the resummed case (at LO and NLO). The NLO resummed curves are given both in the $\text{Q}_0\overline{\text{MS}}$ and in the $\overline{\text{MS}}$ scheme, while at LO-resummed level there is no scheme difference. In fixed order perturbation theory there is no difference between $Q_0\overline{\text{MS}}$ and $\overline{\text{MS}}$ up to and including the NNLO level but $Q_0\overline{\text{MS}}$ and $\overline{\text{MS}}$ become different at higher orders. An important achievement of our work is the complete control of all aspects of scheme change at the resummed level. Resummed results for the splitting function matrix have also been obtained in ref. [26] but in a scheme which differs from the commonly used $\overline{\text{MS}}$ scheme by unknown, presumably small, terms. In contrast our results are given in either the $\text{Q}_0\overline{\text{MS}}$ or the $\overline{\text{MS}}$ schemes in a completely specified way.

We now discuss the main features of the resulting splitting functions. We show the most important of the four, xP_{gg}, in fig. 1. As for the $n_f = 0$ case that we studied in our previous work [15], the difference between the resummed and fixed order LO and NLO curves in the x range relevant for collider experiments is moderate. But the strong instability shown by the NNLO fixed order perturbation theory is cured by the resummation. Above $x \sim 0.1$ the resummed curves match precisely the corresponding fixed order ones. For smaller values of x, the splitting function xP_{gg} shows a significant dip directly inherited from xP_+ [19]. This dip has important phenomenological consequences in that it extends the region of validity of the fixed order perturbative LO and NLO evolution. The onset of the truly asymptotic small x rise, both in the resummed LO and the NLO (in the $\text{Q}_0\overline{\text{MS}}$ scheme) curves, is postponed to very small values of x. Note that for xP_{gg} the $\overline{\text{MS}}$ curves are considerably steeper than in the $\text{Q}_0\overline{\text{MS}}$ scheme at small x. This is the due to the singular nature of the scheme change eq. (4.16) which takes to $\text{Q}_0\overline{\text{MS}}$, whose effects are only compensated when the evolved parton densities are combined with the coefficient functions.
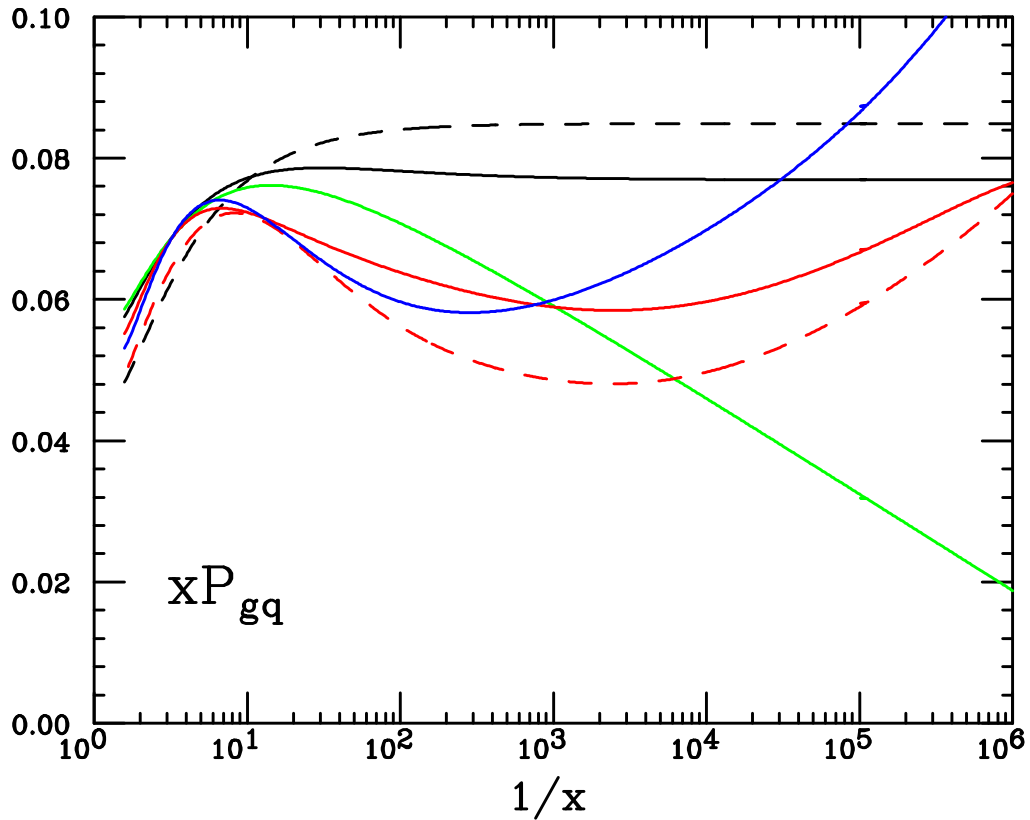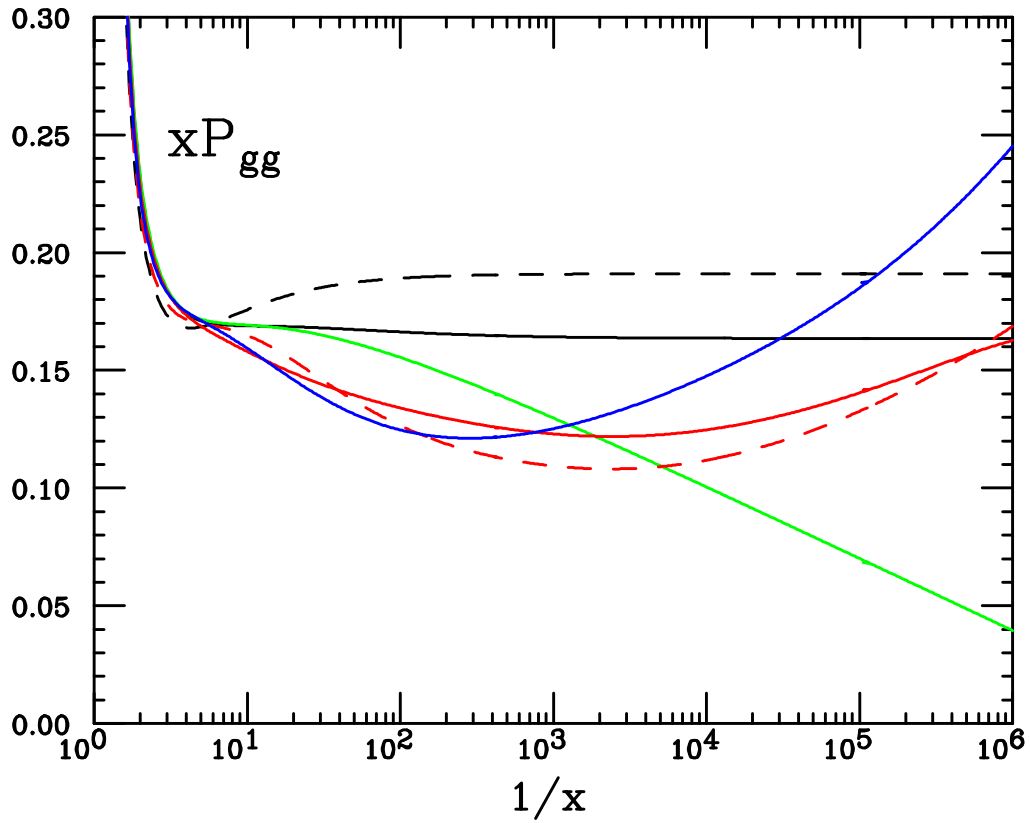
Figure 1: The gluon splitting functions xP_{gg} and P_{gq}, plotted with $\alpha_s = 0.2$ and $n_f = 4$. The curves are (from top to bottom for xP_{gg} at $x \sim 0.2$): fixed order perturbation theory LO (black dashed), NLO (black solid), NNLO (green), resummed LO (red dashed) and NLO in $Q_0\overline{\text{MS}}$ scheme (red solid) and in the $\overline{\text{MS}}$ scheme (blue)
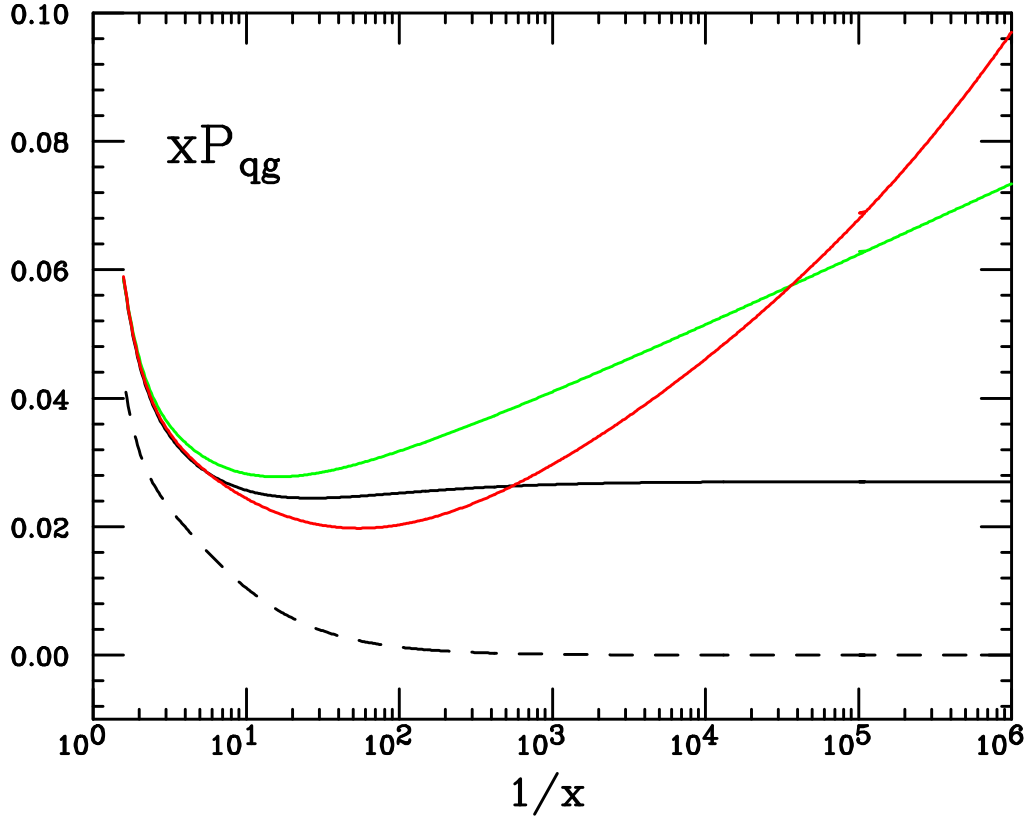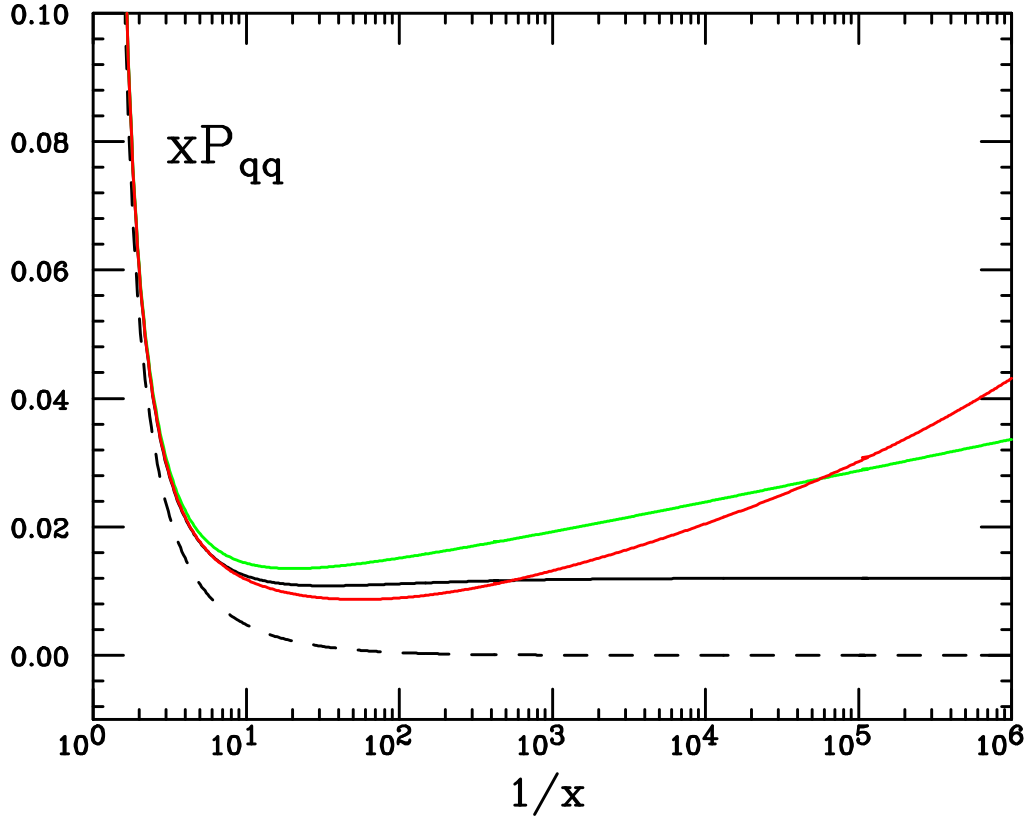
25

Figure 2: The quark splitting functions xP_{qq} and xP_{qg} plotted with $\alpha_s = 0.2$ and $n_f = 4$. The curves are as in fig. 1a (bottom to top for $x \sim 10^{-6}$). Note however that here the resummed LO coincides with unresummed LO, and resummed NLO $\overline{\text{MS}}$ coincides with resummed NLO $Q_0\overline{\text{MS}}$.

The splitting function xP_{gq} is also plotted in fig. 1. It inherits most of the features of xP_{gg}, except that it is very soft at large x. Note that the absolute scale of xP_{gq} is about $\frac{4}{9}$ smaller than that of xP_{gg} at small x, which can be directly attributed to the ratio of colour Casimir factors C_F/C_A.

The singlet quark splitting functions P_{qq} and P_{qg} are shown in fig. 2. Here the resummed LO coincides with the unresummed LO: indeed the resummation effects start at NLO. The NLO resummed curves at not too small values of x are always bracketed between the LO and NNLO perturbative results. Moreover the singular parts of xP_{qq} are again $\frac{4}{9}$ times those of xP_{qg} so that their resulting behaviour is similar. Recall also that, as discussed in sect. 4.2, the $Q_0\overline{\text{MS}}$ scheme has been defined in such a way that xP_{qq} and xP_{qg} are the same as in $\overline{\text{MS}}$.

For the coefficient functions there are four curves in each of the $c_{q,g}^i$ plots in figs. 3-4. The curves refer to the NLO and NNLO fixed order perturbative results (the LO coefficients are either zero or, in the case of c_q^2, proportional to a delta function at $x = 1$: $c_q^2 = \frac{5}{18}\delta(1-x)$) and to the NLO resummed coefficients in the $Q_0\overline{\text{MS}}$ and $\overline{\text{MS}}$ schemes. We see that also for the coefficient functions the $\overline{\text{MS}}$ curves are steeper at small x because in this scheme the contributions corresponding to the singular term eq. (2.18) are included in the coefficient function. For this reason, in our previous papers on the theory of resummed evolution for the singlet structure functions, we always adopted the $Q_0\overline{\text{MS}}$ scheme, where no unphysical singularities appear either in the splitting functions or in the coefficients. In a different scheme the combination of splitting functions and coefficients leads to a compensation in the evolution of physical quantities, which end up being different only through higher order effects, as we shall see later.

In figs. 5-10 we show the separate dependence on n_f and α_s of the splitting functions and coefficients. In practice, the relevant effective values of n_f and of α_s are both functions of Q^2, so that their values move in a correlated way. However, for the sake of illustration, we show here the variation of one while the other is kept fixed.

The n_f dependence of splitting functions and coefficients is displayed in figs 5-7. All these plots are for $\alpha_s = 0.2$. For clarity we only include the fixed order perturbative results at NLO and NNLO, and the resummed ones at NLO in the $Q_0\overline{\text{MS}}$ scheme. The varying n_f plots have $n_f = 3, 4, 5, 6$ (solid) and $n_f = 0$ (dotted) where relevant, for comparison. The plotted curves for the gluon splitting functions (xP_{gg} and xP_{gq}) decrease as n_f increases, while the quark splitting functions (xP_{qq} and xP_{qg}) increase. From these plots we see that varying n_f does not make too much difference for xP_{gg} and xP_{gq}, but the addition of more quarks softens the growth at small x. In the quark sector for splitting functions and for all the coefficient functions, there is an overall factor of n_f in the main logarithmic terms. Thus the leading effect is an approximately linear rise in modulus with n_f at small x; note that the longitudinal NNLO coefficient functions are negative at small x, and become more negative as n_f increases.

The α_s dependences of splitting functions and coefficients are displayed in figs 8-10. The varying α_s plots have $\alpha_s = 0.1$, 0.15, 0.2, 0.25, 0.3. All curves have $n_f = 4$. In the plots the splitting functions and coefficients are multiplied by $0.2/\alpha_s$, so that the linear dependence on α_s is divided out, and the $\alpha_s = 0.2$ curves are the same as those in figs 1-3. At low enough x, all the resummed splitting functions and coefficients
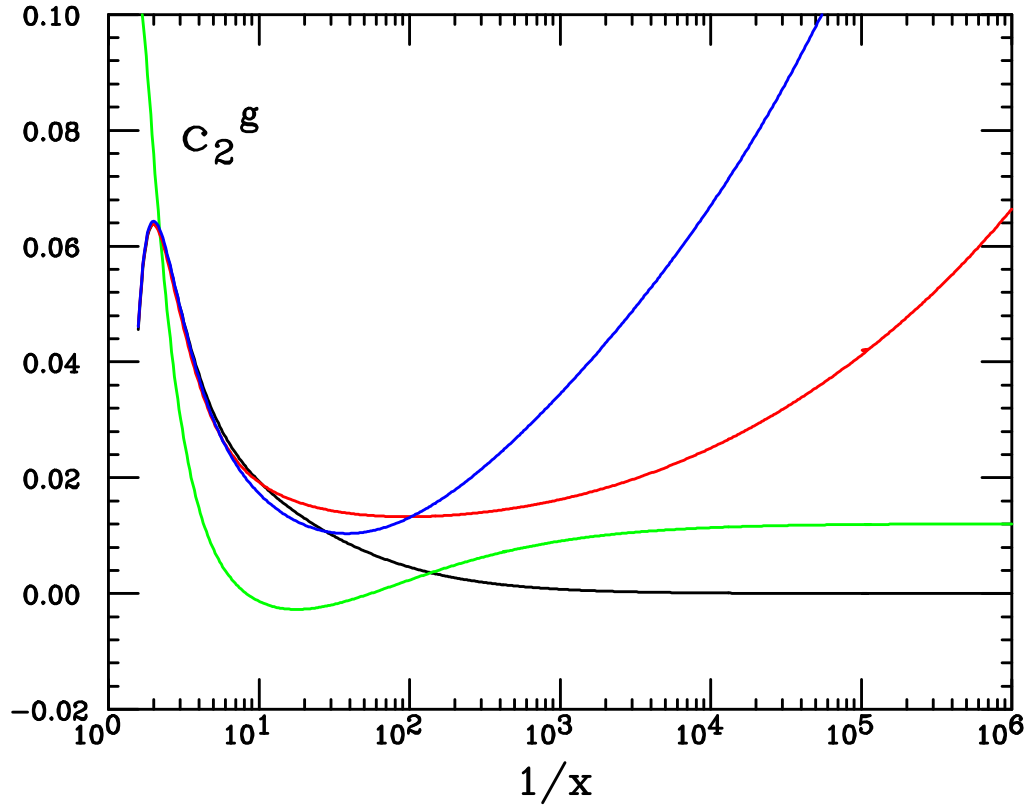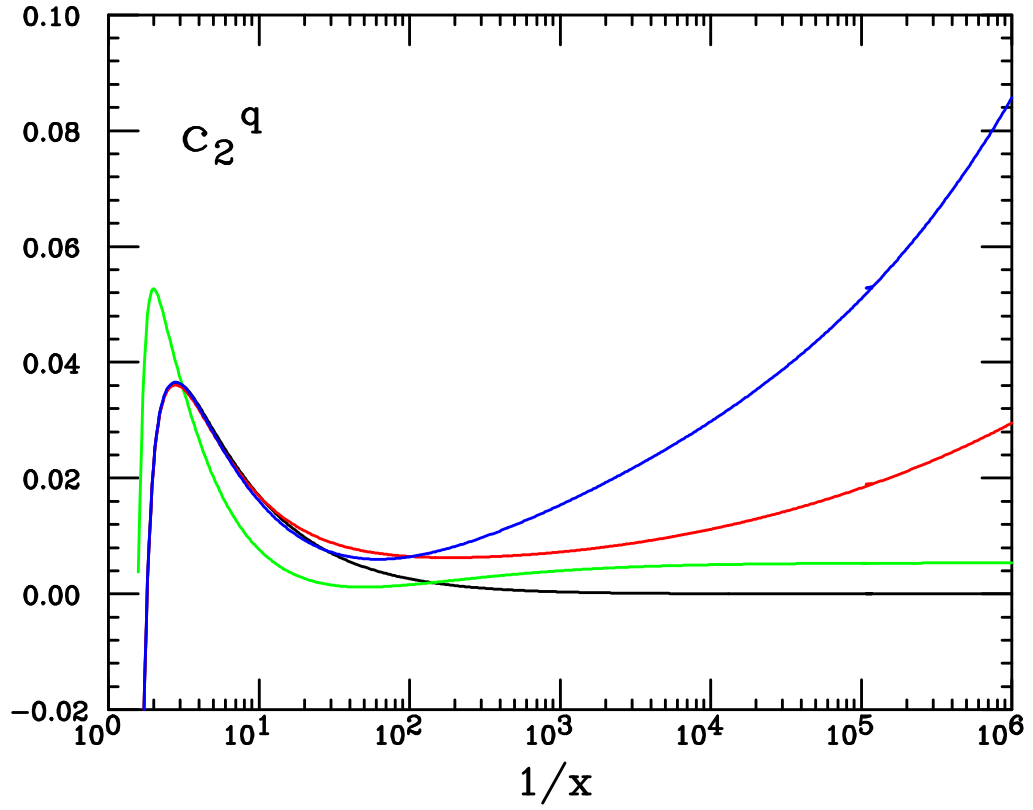
Figure 3: The F_2 coefficients plotted with $\alpha_s = 0.2$ and $n_f = 4$. The curves are (bottom to top for $x \sim 10^{-4}$): fixed order perturbative: NLO (black solid), NNLO (green) resummed NLO (red solid) in $Q_0\overline{MS}$ scheme, resummed NLO in the $\overline{MS}$ scheme (blue).
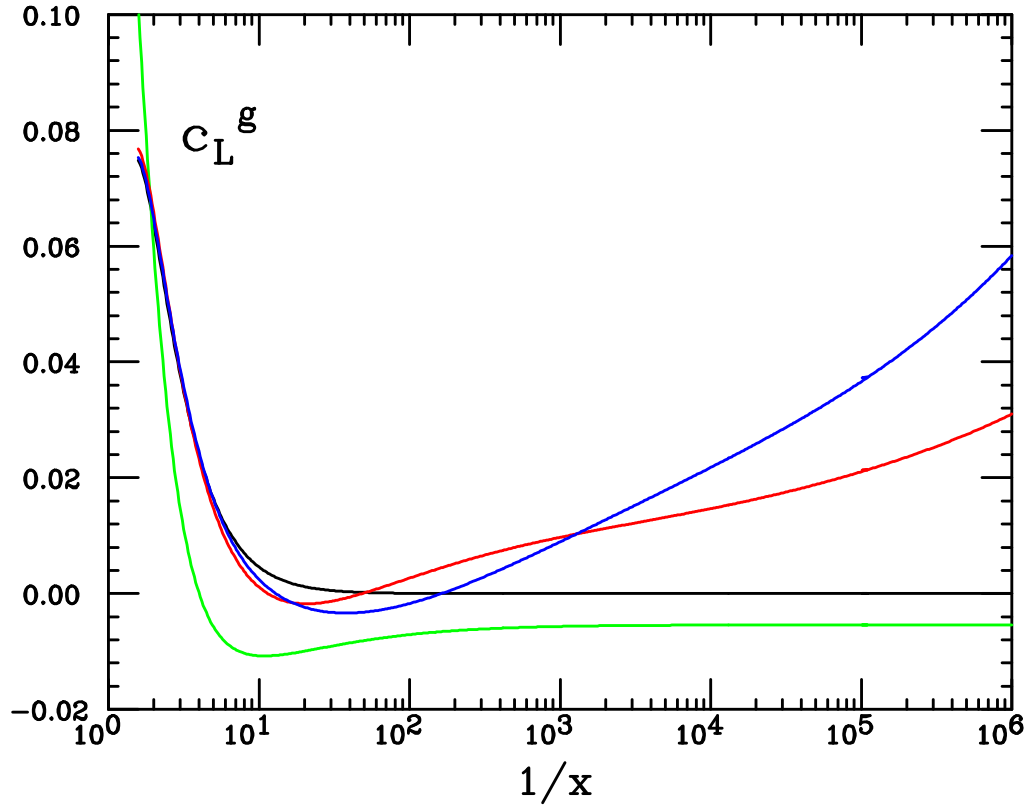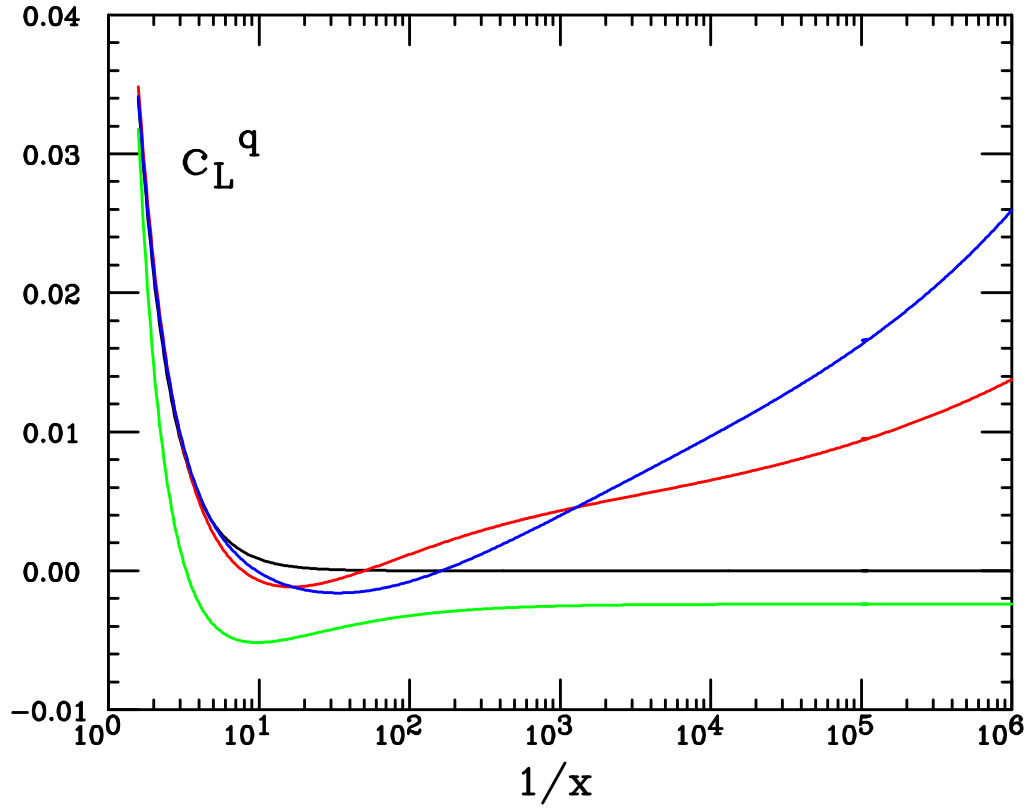
Figure 4: The F_L coefficients plotted with $\alpha_s = 0.2$ and $n_f = 4$. The curves are (bottom to top for $x \sim 10^{-6}$): fixed order perturbative: NNLO (green), NLO (black), resummed NLO (red) in $Q_0\overline{MS}$ scheme, resummed NLO in the $\overline{MS}$ scheme (blue).
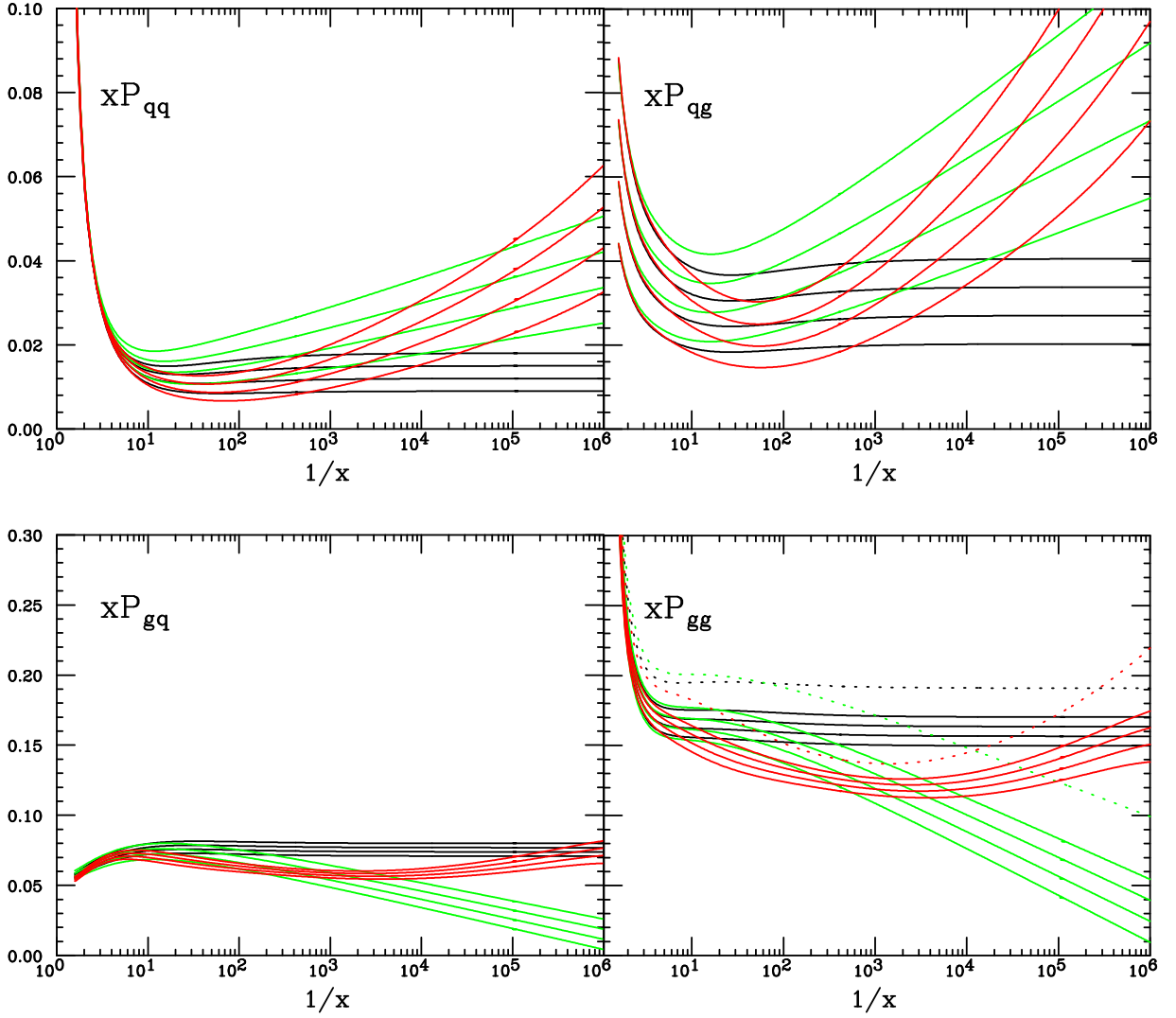
Figure 5: n_f dependence of splitting functions for $\alpha_s = 0.2$. The plotted curves are for $n_f = 3, 4, 5, 6$ (solid), for gg also $n_f = 0$ (dotted) is shown for comparison. The three sets of splitting functions are: fixed order perturbative: NLO (black), NNLO (green); resummed NLO (red) in $Q_0\overline{\text{MS}}$ scheme. For qq and qg as n_f increases the small x value becomes larger: asymptotically constant at NLO, stronger rise at NNLO and strongest rise at the resummed level. For gq and gg as n_f increases the small x value becomes smaller: asymptotically constant at NLO, stronger drop at NNLO and deeper dip at the resummed level.

show a steeper increase as α_s increases. This is because the leading singularity in the N plane moves further to the right making the asymptotic behaviour steeper at small x. At the same time xP_{gg}/α_s and xP_{gq}/α_s decrease in the intermediate region (i.e. the dip gets deeper). The rate of increase at small x and the depth of the dip are related by a smooth interpolation between small and large x and because of the integral constraint from momentum conservation (although the delta function terms at $x = 1$ also depend on α_s). The NNLO results, shown for comparison, as α_s increases display a steeper rise at small x of splitting functions in the quark sector and a steeper drop in the gluon sector,
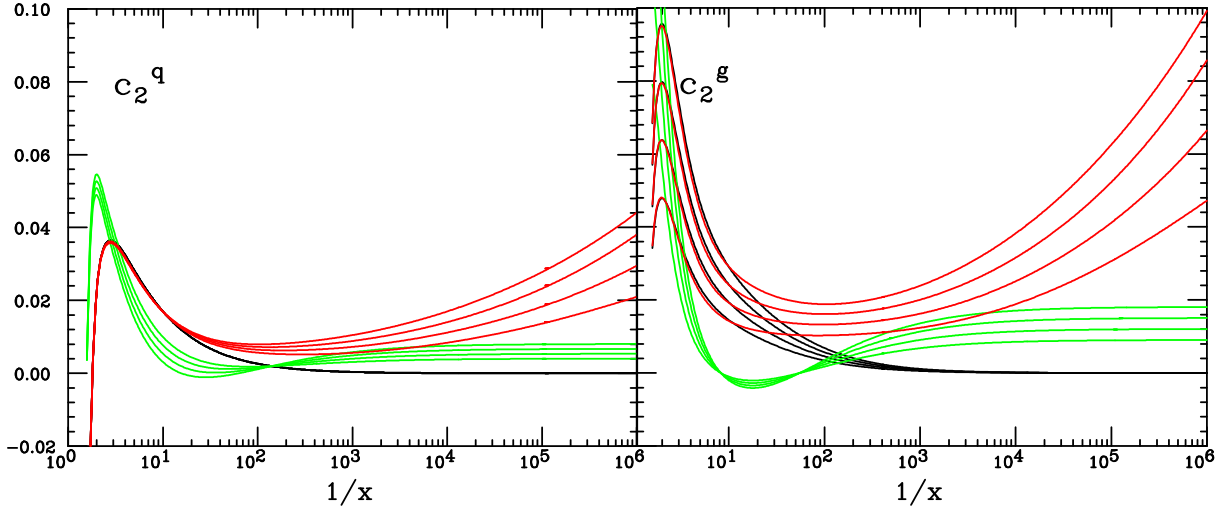
Figure 6: The n_f dependence of F_2 coefficients for $\alpha_s = 0.2$. The plotted curves are for $n_f = 3, 4, 5, 6$ (solid). The three sets of coefficients are: fixed order perturbative: NLO (black), NNLO (green); resummed NLO (red) in $Q_0\overline{\text{MS}}$ scheme. Note that the fixed order perturbative NLO result is independent of α_s. In all cases, for both q and g, there is an increase with n_f at small x.
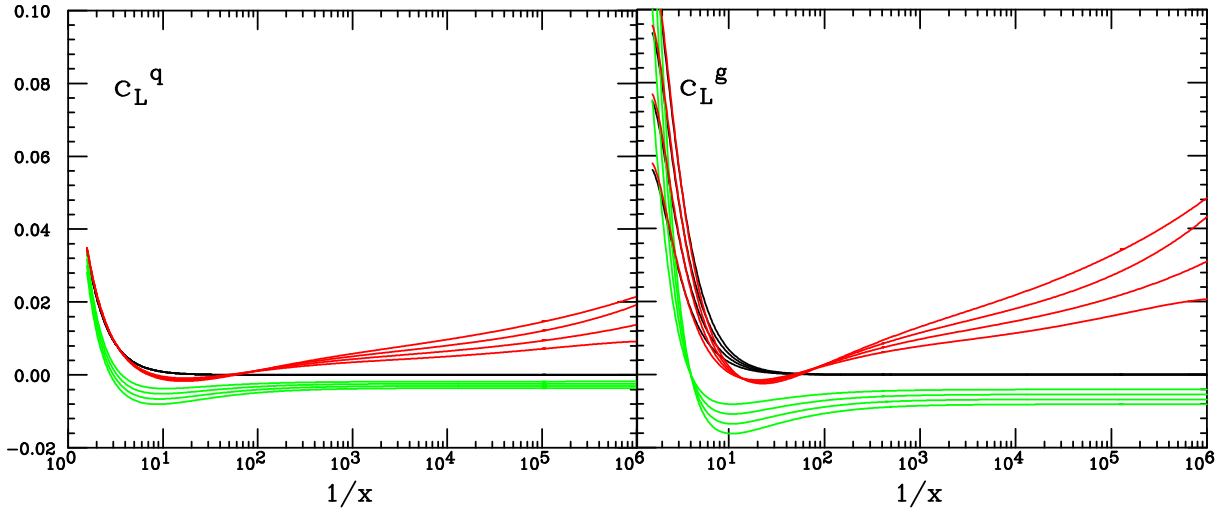

Figure 7: As fig. 6, but now the n_f dependence of F_L coefficients. In all cases, for both q and g, there is an increase in modulus with n_f at small x, the resummed result being positive while the fixed NNLO is negative.

and coefficient functions which, while remaining asymptotically flat at small x, become larger in modulus (positive for c_2 and negative for c_L) Comparing results at the NNLO fixed order perturbative level with the resummed result at the NLO level, one sees that the resummation improves the stability of the splitting functions even at rather large α_s.

5.2. Parton distributions and structure functions

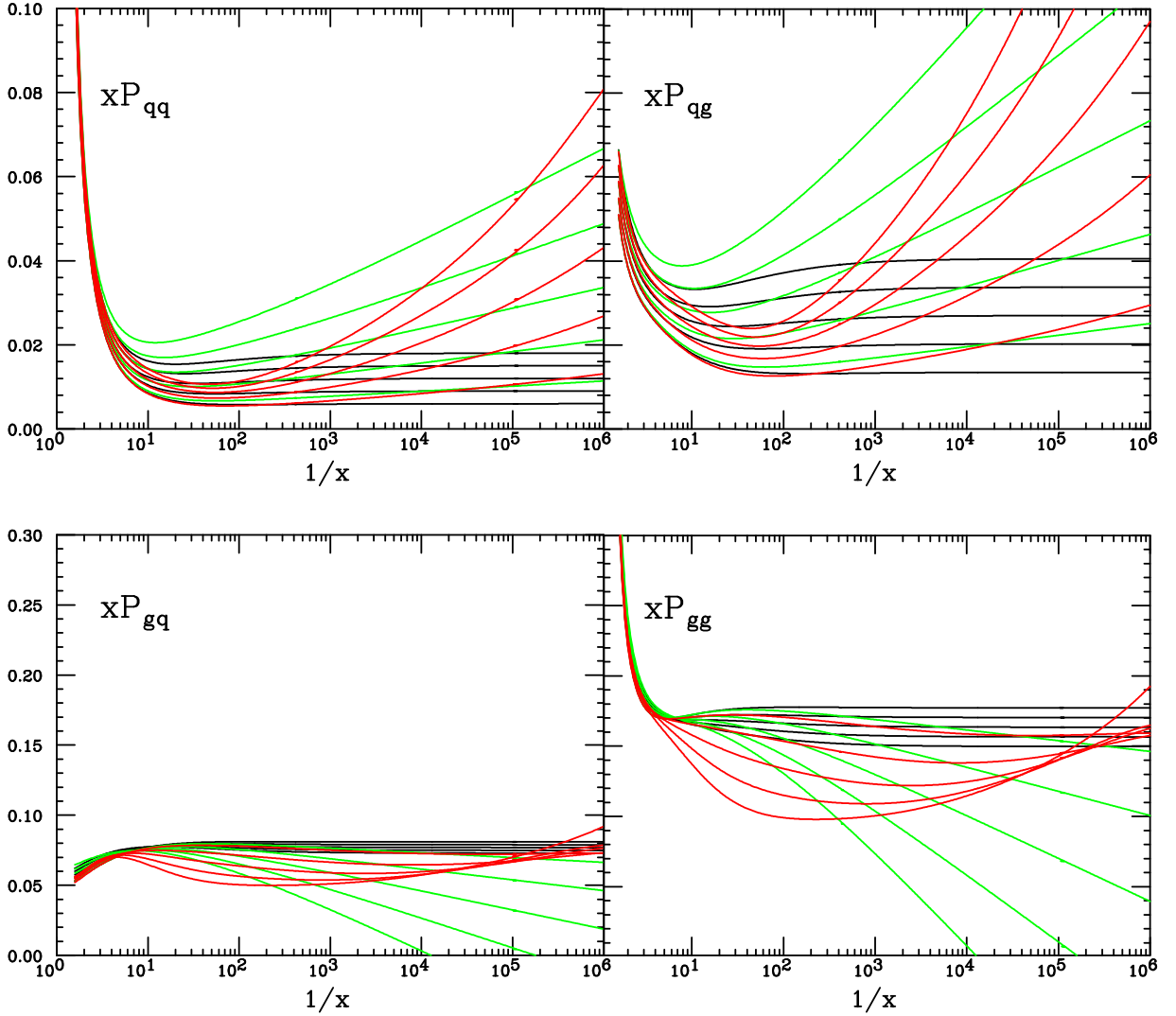We now discuss the resulting evolution of parton densities and of structure functions

Figure 8: α_s dependence of splitting functions for $n_f = 4$. All curves are rescaled by $0.2/\alpha_s$, in order to eliminate the proportionality to α_s. The values of α_s are $\alpha_s = 0.1, 0.15, 0.2, 0.25, 0.3$. The three sets of splitting functions are: fixed order perturbative: NLO (black), NNLO (green); resummed NLO (red) in $Q_0\overline{\mathrm{MS}}$ scheme. At the resummed level, for qq and qg there is an increase with α_s at small x, while for gq and gg a decrease at small x and a deeper dip. At NNLO as α_s increases there is a steeper rise for qq and qg and a steeper drop for gq and gg.

and compare the resummed curves with the corresponding fixed order perturbative ones. In these plots α_s is running with Q^2 with $\alpha_s(m_Z) = 0.118$. The value of n_f is varied according to the zero–mass variable variable flavour number scheme: contributions from heavy quarks vanish below threshold and are generated dynamically by perturbative evolution above threshold. In figs. 11-12 we show the gluon and singlet quark parton densities as a function of x, down to $x = 10^{-6}$, at different values of $Q = 2, 4, 10, 100, 1000$ GeV. The initial parton densities at $Q_0 = 2$ GeV are chosen to have a typical simple semi-realistic shape, adequate for our present purposes. Namely, we take [10]:

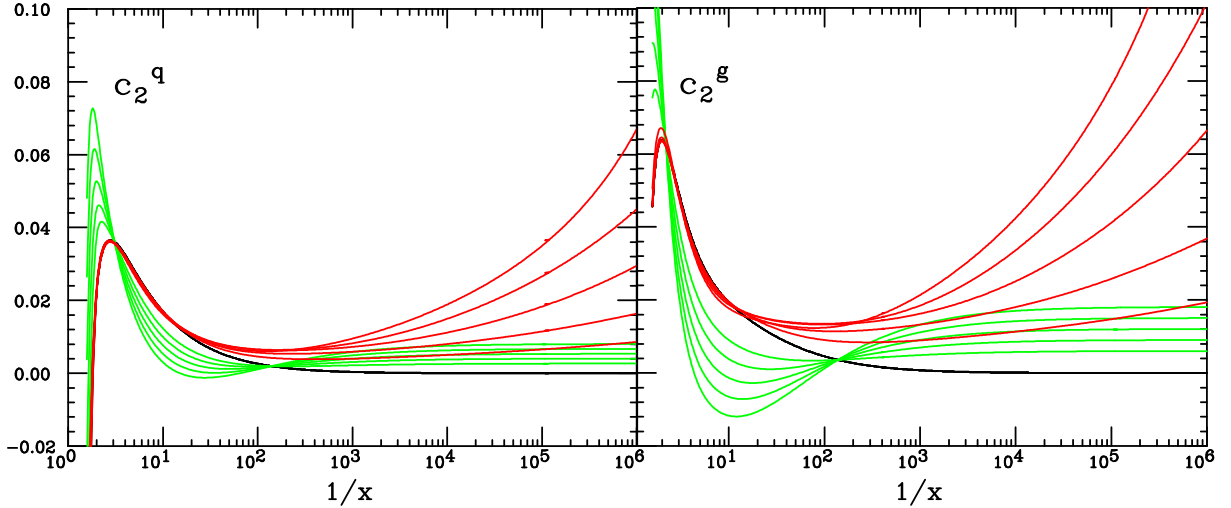$$xg(x, t_0) = r_s x q_{sea}(x, t_0) = k_g x^{-0.18}(1 - x)^5, \tag{5.1}$$

32

Figure 9: The α_s dependence of F_2 coefficients. All curves are rescaled by $0.2/\alpha_s$, in order to eliminate the proportionality to α_s. The values of α_s are $\alpha_s = 0.1, 0.15, 0.2, 0.25, 0.3$. The three sets of coefficients are: fixed order perturbative: NLO (black: note that the result only depends on n_f for c_2^g), NNLO (green); resummed NLO (red) in $Q_0\overline{MS}$ scheme. For both coefficients there is in all cases an increase with α_s at small x. The resummed curves rise at small x while the NLO and NNLO ones are asymptotically constant.
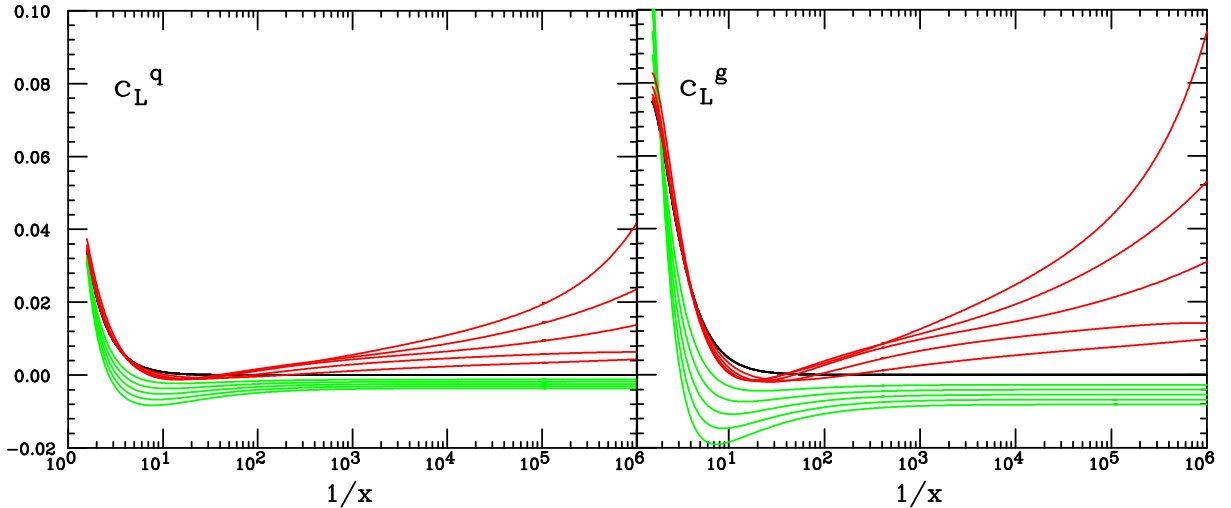
Figure 10: As in fig. 9, but now the α_s dependence of the F_L coefficients. For both coefficients at small x there is an increases with α_s in the resummed case (steeper growth) and a decrease with α_s at NNLO (smaller negative asymptotic constant).

$$xq_v(x, t_0) = k_q x^{0.5}(1-x)^4, \tag{5.2}$$

where $t_0 = \ln Q_0^2/\mu^2$. The constants k_g and k_q are fixed in such a way that the valence and momentum sum rules are satisfied. We choose $r_s = 3$, so the fractions of momentum at $Q = Q_0$ are 28% for valence quarks, 18% for sea quarks and 54% for gluons.

The plots show, separately for the gluon and the total singlet quark densities, the
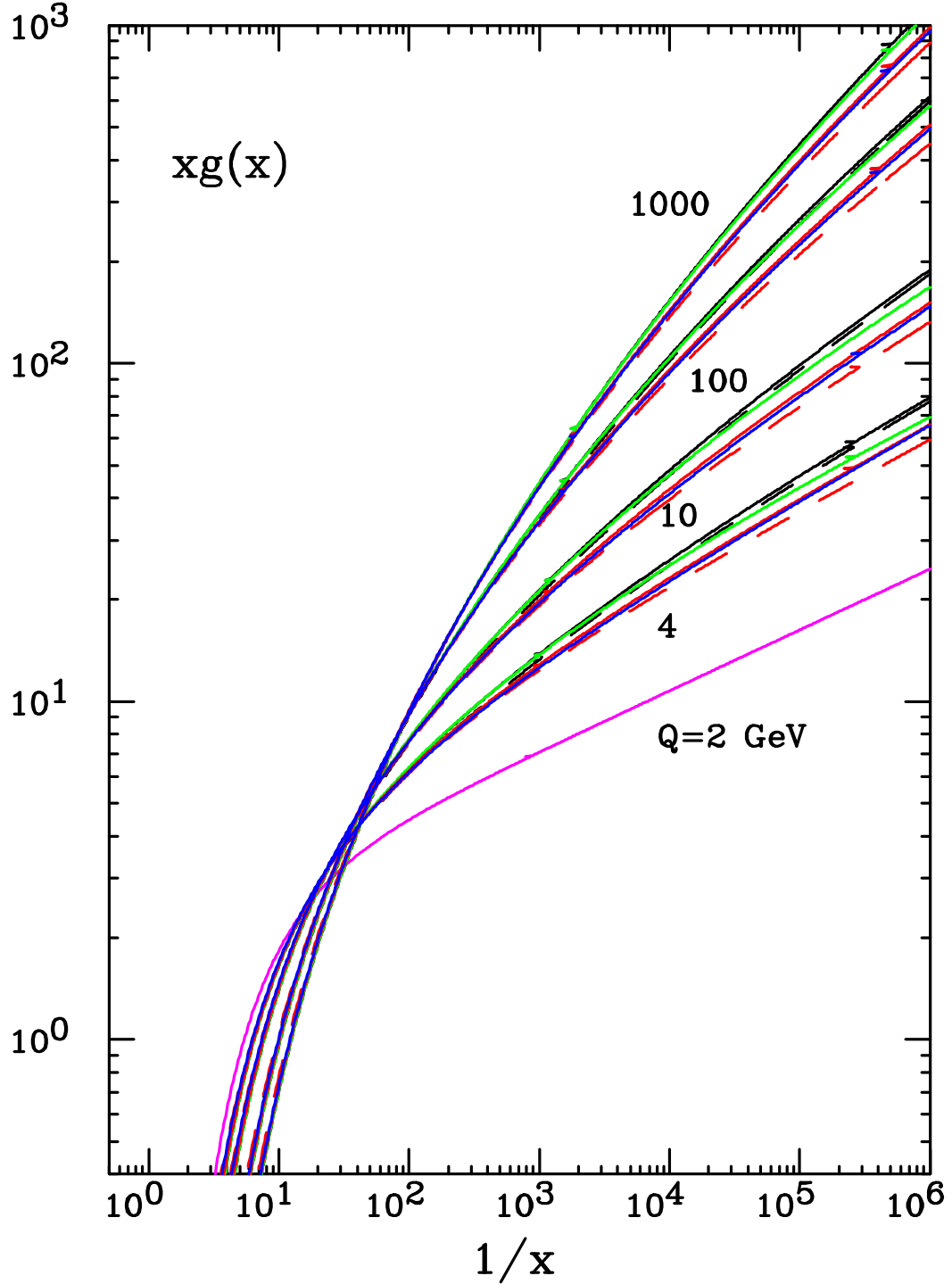
33

Figure 11: The small x behaviour of the gluon distribution as a function of $1/x$ at different values of $Q = 4$, 10, 100, 1000 GeV (for $\alpha_s = 0.2$ and $n_f = 4$). Also shown (purple) the initial parametrization at $Q = 2 \ GeV$. The curves are: fixed order perturbation theory LO (black dashed), NLO (black solid), NNLO (green); resummed LO (red dashed) and NLO (red solid) in $Q_0\overline{\rm MS}$ scheme resummed NLO (blue solid) in the $\overline{\rm MS}$ scheme. At all scales the fixed NLO curve is highest (fixed LO slightly lower), the NNLO is lower, and the resummed NLO is lowest (resummed LO yet slightly lower). Note that the blue and red curves (resummed NLO in the two schemes) are almost indistinguishable.
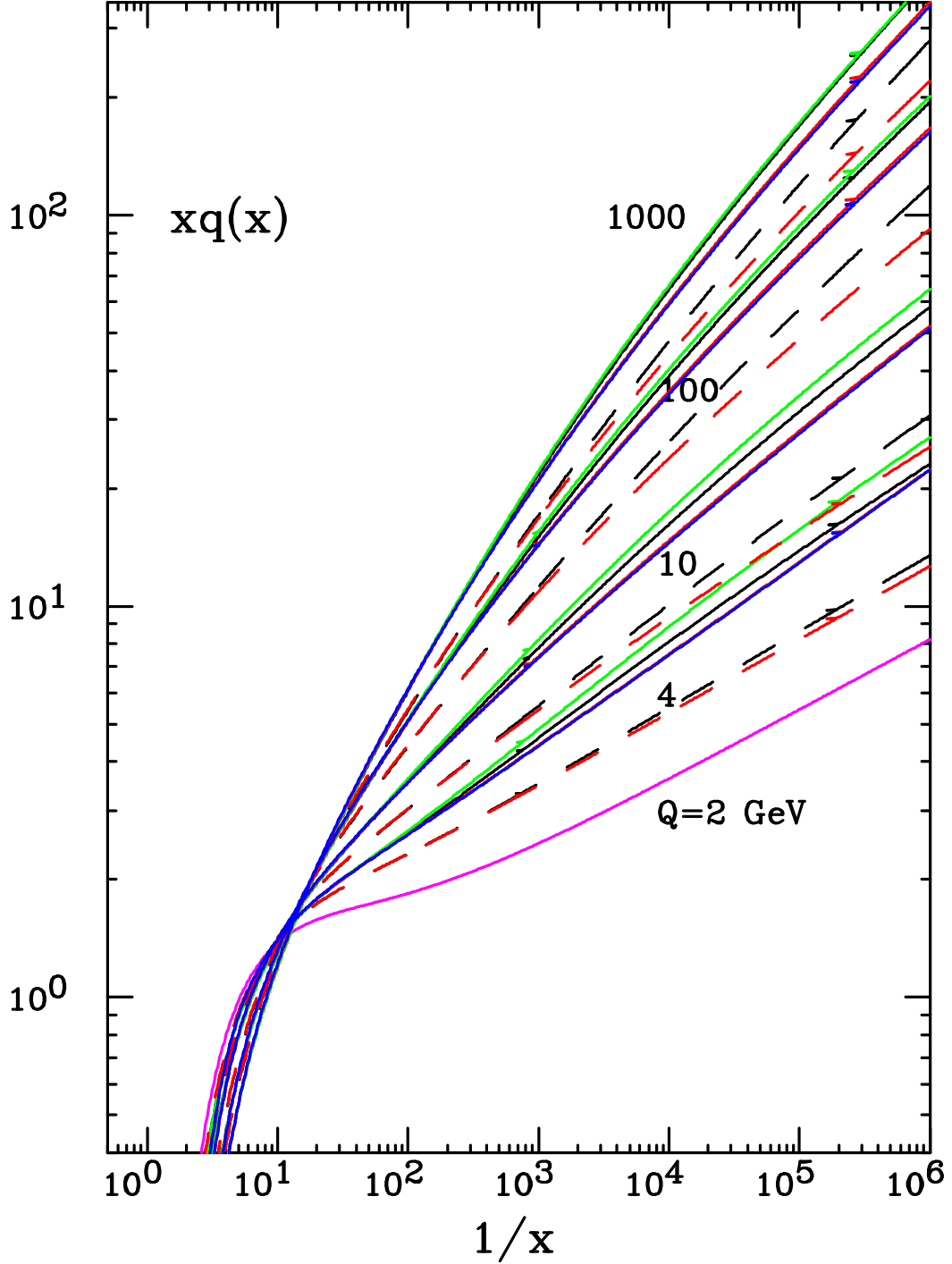
34

Figure 12: The small x behaviour of the total (valence plus sea) singlet quark distribution as function of $1/x$ at different values of $Q = 4,\ 10,\ 100,\ 1000$ GeV (for $\alpha_s = 0.2$ and $n_f = 4$). Also shown (purple) the initial parametrization at $Q = 2$ GeV. The curves are: fixed order perturbation theory LO (black dashed), NLO (black solid), NNLO (green); resummed LO (red dashed) and NLO (red solid) in $Q_0\overline{\text{MS}}$ scheme resummed NLO (blue solid) in the $\overline{\text{MS}}$ scheme. At all scales, the LO curves are lowest (resummed below fixed order), resummed NLO higher, fixed NLO yet higher and fixed NNLO highest. Note that the blue and red curves (resummed NLO in the two schemes are almost indistinguishable.

35

initial distributions at $Q_0 = 2$ GeV, and then, for each higher value of Q, the resulting evolved distributions in the fixed order perturbative case, at LO, NLO and NNLO accuracy, and in the resummed case at LO and NLO (the latter both in the $Q_0\overline{\text{MS}}$ and $\overline{\text{MS}}$ schemes). At small x there is less evolution in the resummed cases than in fixed order perturbation theory. This is a consequence of the dip in the splitting functions. In all cases the scheme dependence in the resummed NLO case is not very important.

We have also studied the renormalization scale dependence of the gluon and singlet quark evolution at fixed x and t, by letting

$$f(x,t;k) = f(x,t+\ln k) - \ln k \frac{d}{dt}f(x,t+\ln k) + \tfrac{1}{2}\ln^2 k \frac{d^2}{dt^2}f(x,t+\ln k), \qquad (5.3)$$

where $f(x,t)$ is the quark or gluon distribution. At LO (fixed–order or resummed) only the first contribution on the right–hand side is included; at NLO we include the first term evaluated at NLO, and the second evaluated at LO, while at NNLO we keep the first term evaluated at NNLO, the second evaluated at NLO and the third evaluated at LO. It is easy to show that this is equivalent to the usual formulation of renormalisation scale variation where the argument of the running coupling in the evolution equations is changed from Q^2 to kQ^2.

The scale variation eq. (5.3) provides an estimate of the size of the theoretical uncertainty related to higher order contributions to evolution equations, provided the expansion itself is uniform in x. Hence, we expect it to provide a reliable estimate at the resummed level, and to underestimate uncertainties at NLO and NNLO fixed order, where scale variation cannot include the effect of higher–order logarithmic terms. For example, in a NNLO fixed order calculation, scale variation explores the effect of subleading contributions to xP_{gg} of the form $\alpha_s^4 \ln x$, but fails to see the (known) $\alpha_s^4 \ln^3 x$ contribution, which at small x is of course much larger.

In fig. 13 we plot the evolved gluon density (starting from $Q_0 = 2$ GeV as described above) with k eq. (5.3) varied between 0.1 and 10 at fixed $Q = 10$ GeV and $x = 10^{-2}$, 10^{-4} or 10^{-6}. The scale dependence is larger at smaller values of x where the Q^2 dependence is also steeper. The NLO approximations are much more stable against scale change than the LO counterparts, both for resummed and fixed order evolution, in agreement with expectations. The fixed order NNLO shows comparatively little scale dependence, but as already mentioned this does not include the effect of higher–order logs.

Figures 11-12 explore the effects of various treatments of perturbative evolution when the input parton distribution is kept fixed. However, when higher–order corrections and resummation are consistently included, the input physical observables are fixed and the parton distributions are refitted. Hence, a more realistic estimate of the physical impact of the corrections can be obtained by assuming that some physical observables are kept fixed (for example, the structure functions F_2 and F_L) at a given scale, parton distributions are determined from them, and then these parton distributions are used to compute new physical observables (for example, structure functions or hadronic cross-sections at a higher scale).

In practice, we proceed as follows. We write the structure functions $F(N,t)$ eq. (3.1) as the product eq. (3.2) of a matrix coefficient function $c(x, \alpha_s(t))$ eq. (3.3) and an evolution
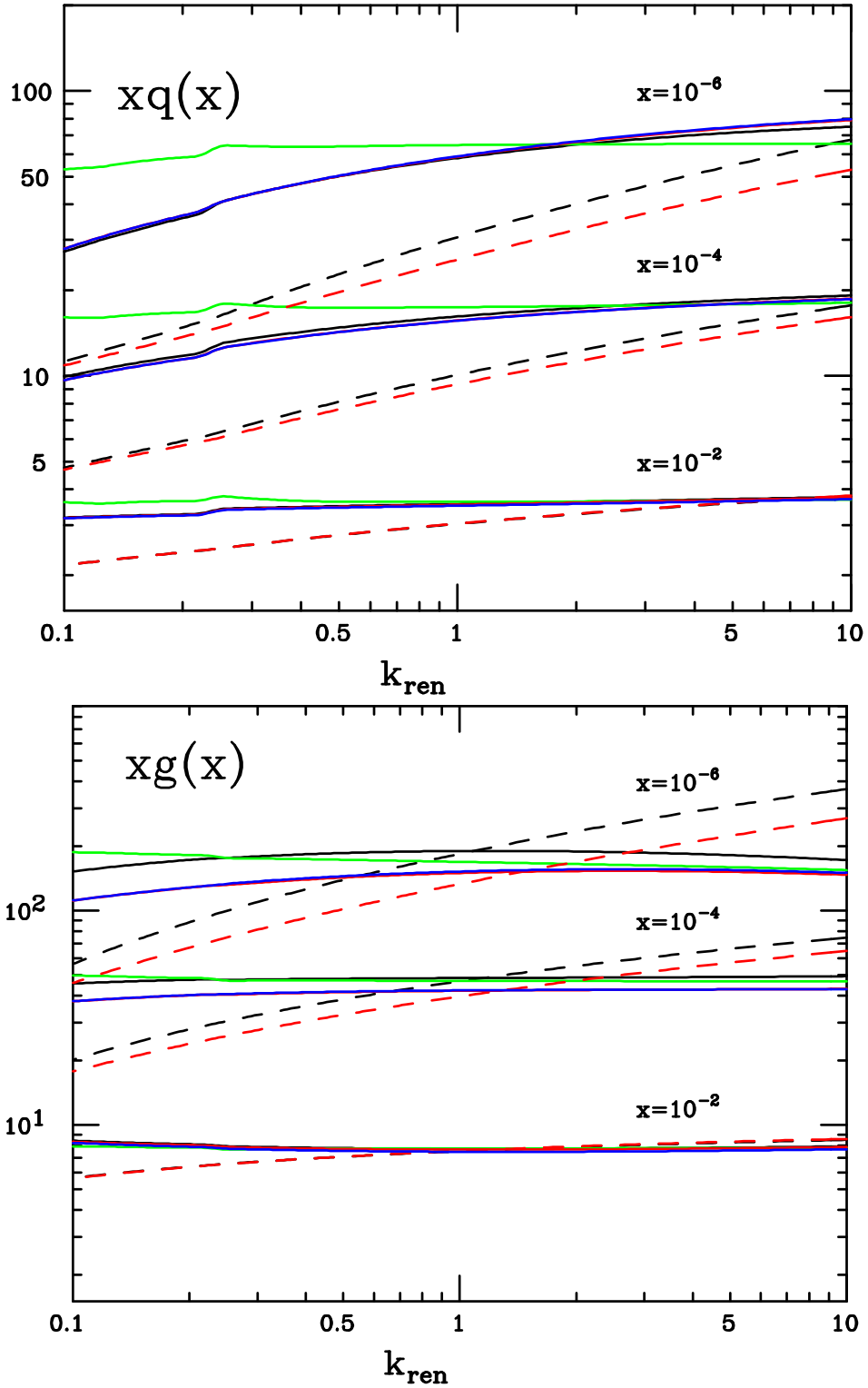
Figure 13: The renormalization scale dependence eq. (5.3) of the singlet quark and of the gluon parton densities at fixed $Q = 10$ GeV and $x = 10^{-2}$ or 10^{-4} or 10^{-6} (with $n_f = 4$). The curves are: fixed order perturbation theory LO (black dashed), NLO (black solid), NNLO (green); resummed LO (red dashed); resummed NLO in $Q_0\overline{\mathrm{MS}}$ scheme (red solid) and in $\overline{\mathrm{MS}}$ scheme (blue solid).

37

factor $\Gamma(N, t, t_0)$ eq. (3.11), times some initial parton distribution $f(N, t_0)$:

$$F(N, t) = c(N, \alpha_s(t))\Gamma(N, t, t_0)f(N, t_0). \tag{5.4}$$

We then determine the structure functions at $Q_0 = 2$ GeV using the parton distributions eq. (5.1)-(5.2) and the fixed order NLO expressions of the coefficient functions:

$$F_{\mathrm{NLO}}(N, t_0) = c_{\mathrm{NLO}}(N, \alpha_s(t_0))f(N, t_0). \tag{5.5}$$

Finally, we compute structure functions with various fixed–order and resummed choices form the coefficient functions and anomalous dimensions (and thus evolution factor), and with the input redefined in such a way that at Q_0^2 all the structure functions are the same. So for instance at the resummed level we used resummed expressions of the coefficient function and evolution factor, and take as redefined input

$$f_{\mathrm{res}}(N, t_0) = C_{\mathrm{res}}^{-1}(N, \alpha_s(t_0))F_{\mathrm{NLO}}(N, t_0). \tag{5.6}$$

so that since

$$F_{\mathrm{res}}(N, t) = C_{\mathrm{res}}(N, t)f_{\mathrm{res}}(N, t_0), \tag{5.7}$$

$F_{\mathrm{res}}(N, t_0) = F_{\mathrm{NLO}}(N, t_0)$.

In fig. 14 we show the K-factors defined as the ratio of the NNLO fixed order or NLO resummed to the NLO fixed order results for the singlet F_2 and F_L structure functions, computed as a function of x by Mellin inversion of the expression eq. (5.4) with the input parton distribution eq. (5.6). We show results at fixed $x = 10^{-2}$, 10^{-4} or 10^{-6} as function of Q in the range $Q = 2 - 1000$ GeV, with α_s running and n_f varied in a zero–mass variable flavour number scheme as discussed above. The breaks in the curves correspond to the b and t quark thresholds and are a consequence of the zero–mass approximation; in a more refined treatment they would be replaced by a suitable matching at the heavy quark thresholds. For each x value we present three curves: the resummed case in the $Q_0\overline{\mathrm{MS}}$ scheme, the corresponding plot in the $\overline{\mathrm{MS}}$ scheme, and the NNLO fixed order perturbative. The residual moderate scheme dependence between the $Q_0\overline{\mathrm{MS}}$ and the $\overline{\mathrm{MS}}$ results, which is left after combining coefficients and parton densities, is only visible because of the expanded linear scale of these plots, and is much smaller than the scheme dependence of coefficients and parton densities, as was shown in figs. 2 and 3. It is interesting to observe that for F_2 the effect of resummation, at sufficiently small x values, goes in the opposite direction to the NNLO perturbative evolution: the resummed K-factor is less than 1, corresponding to a smaller structure function at higher scales than with fixed order perturbative NLO evolution.

We have determined the factorization scale dependence of the structure functions computed in this way, defined as

$$F(x, t; k) = F(x, t + \ln k) - \ln k \frac{d}{dt} F(x, t + \ln k) + \tfrac{1}{2} \ln^2 k \frac{d^2}{dt^2} F(x, t + \ln k), \tag{5.8}$$

where $F(x, t)$ is the structure function F_2 or F_L. Just as in eq. (5.3), at LO only the first contribution on the right–hand side is included; at NLO we include the first term
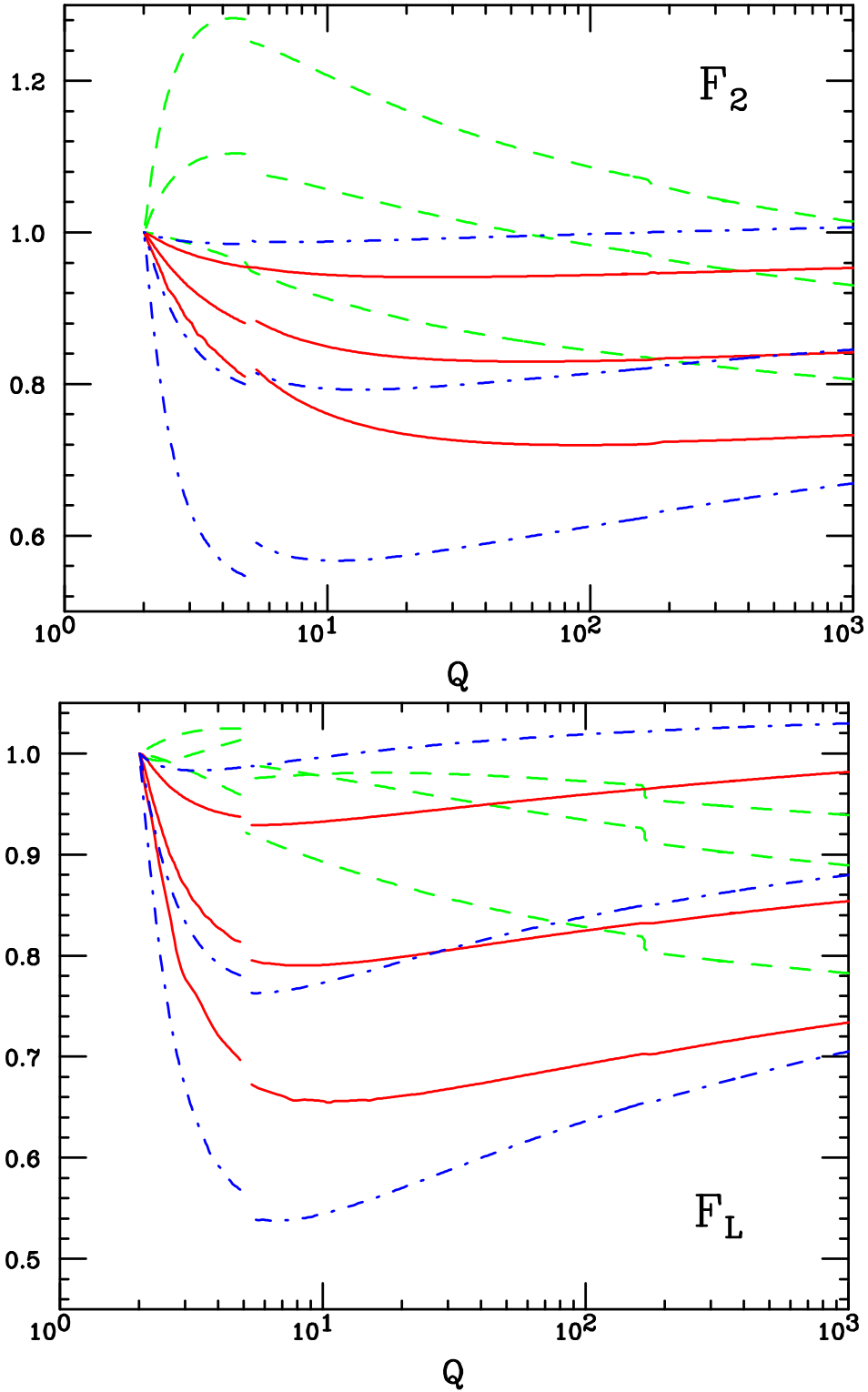
Figure 14: The K-factors, defined as the ratio of the fixed order NNLO or resummed to the NLO fixed order for the singlet F_2 and F_L structure functions, with F_2 and F_L kept fixed for all x at $Q_0 = 2$ GeV. Results are shown at fixed $x = 10^{-2}$, 10^{-4} or 10^{-6} as function of Q in the range $Q = 2 - 1000$ GeV with α_s running and n_f varied in a zero–mass variable flavour number scheme. The breaks in the curves correspond to the b and t quark thresholds. The curves are: fixed order perturbation theory NNLO (green, dashed); resummed NLO in $Q_0\overline{\mathrm{MS}}$ scheme (red, solid), resummed NLO in the $\overline{\mathrm{MS}}$ scheme (blue, dotdashed).
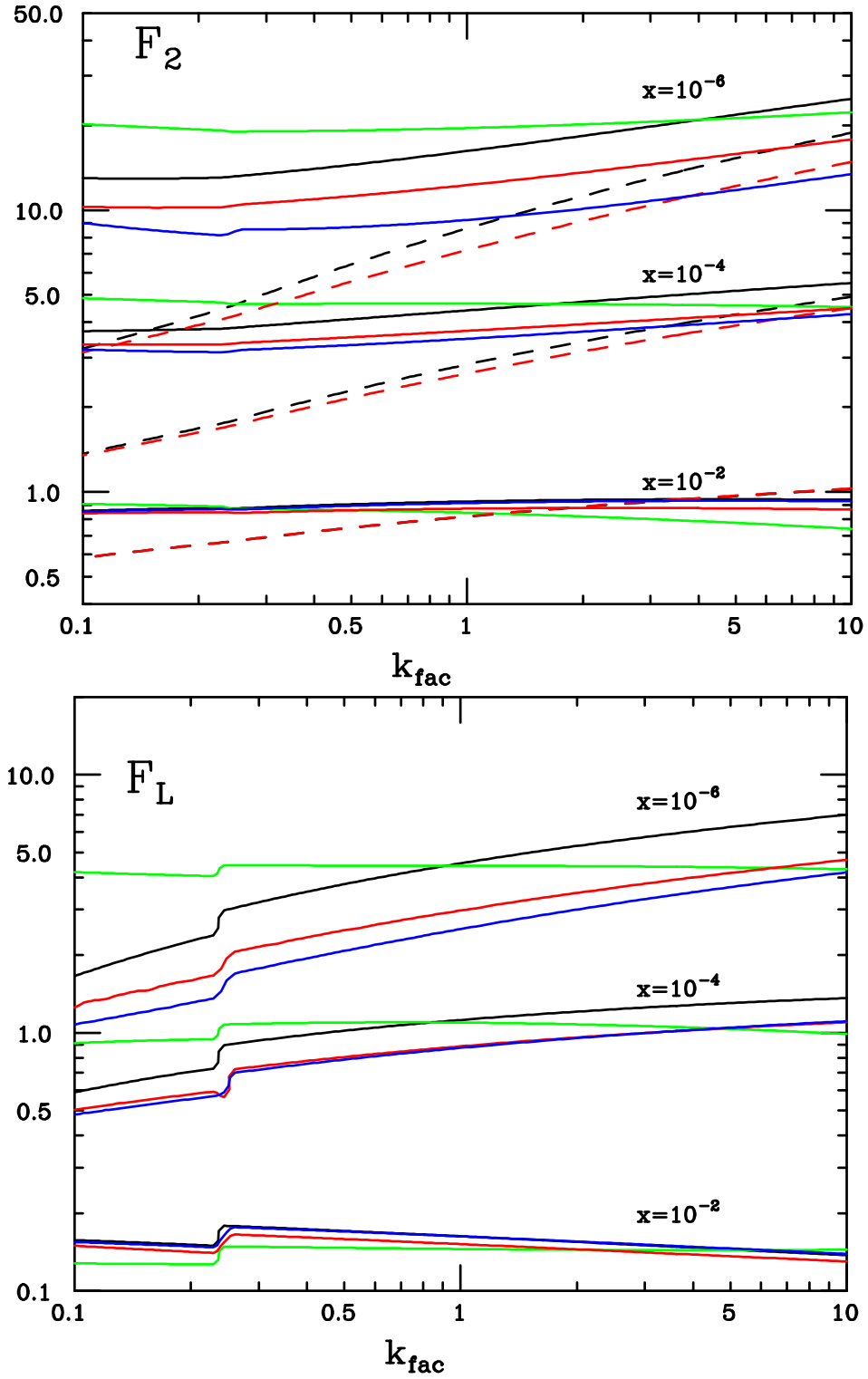
Figure 15: The factorisation scale dependence eq. (5.7) of the singlet F_2 and F_L structure functions at fixed $Q = 10$ GeV and $x = 10^{-2}$, 10^{-4} or 10^{-6} (with $n_f = 4$). The curves are: fixed order perturbation theory LO (black dashed, only F_2), NLO (black solid), NNLO (green); resummed LO (red dashed, only F_2) and NLO (red solid) in $Q_0\overline{\text{MS}}$ scheme resummed NLO (blue solid) in the $\overline{\text{MS}}$ scheme.

40

evaluated at NLO, and the second evaluated at LO, while at NNLO we keep the first term evaluated at NNLO, the second evaluated at NLO and the third evaluated at LO. It is easy to show that this procedure is equivalent to the usual one in which the factorization scale is changed from Q^2 to kQ^2. Results are shown in fig. 15. The general behaviour is similar as that of renormalization scale variation in particular of for singlet quark densities. However, F_2 displays less scale dependence than for quarks, thereby demonstrating the cancellation of scheme dependence between coefficient function and evolution factor. The scheme dependence observed in the difference between the $Q_0\overline{MS}$ and $\overline{MS}$ curves is consistent with the uncertainty obtained from the corresponding scale dependence.

Finally, in order to assess the variation in parton distributions when structure functions are kept fixed, we have computed K-factors for xq and xg when these are determined by evolving up an input determined using eq. (5.6). The K factors are always defined as the ratio of fixed order NNLO or resummed to the NLO fixed order result. In fig. 16 we display these K-factors at fixed $x = 10^{-4}$ or 10^{-6} as function of Q in the range $Q = 2 - 1000$ GeV, with α_s running and n_f varied, when F_2 and F_L are fixed at three different reference scales: $Q_0 = 2$, 5, 10 GeV (the corresponding curves can be identified by the point where the plot starts). These plots compare the effects of evolution with and without resummation when the quark and gluon parton densities extracted at HERA, for example, at $x = 10^{-4}$ and $Q_0 = 5$ GeV, are evolved at the same x value up to, for example, $Q = 100$ GeV for application to LHC phenomenology.

Different important aspects can be observed from these plots. First, one can see the importance of resummation in extracting the parton densities from a given set of data at a given Q. It is well known that the data at smallest x are obtained at smallest Q on the average. Thus, for example, for $x = 10^{-6}$ the most relevant curves would be those at $Q_0 = 2$ GeV. We see that, of course, from the same data on structure functions one extracts different values of the parton densities at the reference scale, depending on the perturbative order and whether or not one resums. Also, these different initial parton densities evolve in different ways. We can study this evolution, using the appropriate splitting functions, up to the LHC domain, e.g at $Q = 100$ GeV. We see that the evolution acts in the direction of decreasing the initial differences. In fact, if we had the data at the LHC and we could extract the parton densities directly at $Q = 100$ GeV, the spread would necessarily be much smaller, because $\alpha_s(t)$ is smaller, and the resummation effects would be less important. Thus the evolution, in a consistent way, tends to reduce the differences obtained at smaller values of Q. The general conclusion is that, if resummation effects are disregarded, the associated error in evolving the parton densities from HERA to the LHC is of the order of $5 - 20\%$. Note that the NNLO corrections and the resummed ones go in opposite directions, thus amplifying their difference. Of course, for the computation of physical quantities then also the hard partonic cross-section must be resummed and this would lead to an enhancement which partially compensates for the parton density suppression. Finally, fig. 16 clearly shows that the scheme dependence is moderate, while the resummation effects are rapidly becoming large at small x.
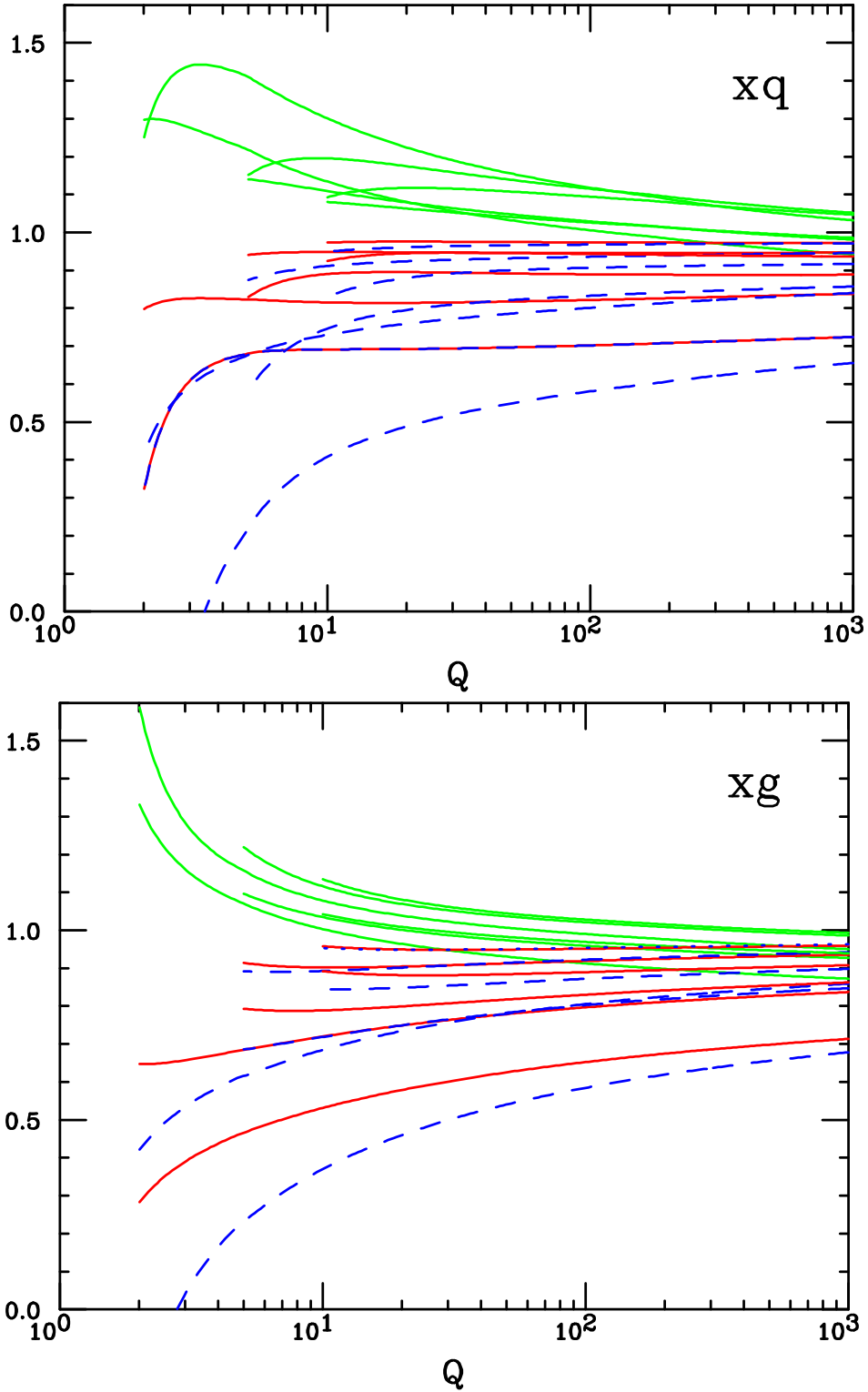
Figure 16: The K-factors, defined as the ratio of the fixed order NNLO or resummed to the NLO fixed order result, for xq and xg at fixed $x = 10^{-4}$ or 10^{-6} as function of Q in the range $Q = 2 - 1000 \; GeV$, with α_s running and n_f varied, when F_2 and F_L are fixed, eq. (5.6), at three different reference scales: $Q_0 = 2, \; 5, \; 10 \; GeV$. The starting scale can be identified by the point where the curves start. The curves are: fixed order perturbation theory NNLO (green, $K > 1$ at low scale); resummed NLO in $Q_0\overline{MS}$ scheme (red), resummed NLO in the $\overline{MS}$ scheme (blue dashed).

6. Conclusion

We have by now achieved a good understanding of the behaviour of singlet structure functions and of their evolution at small x well beyond the domain explored at HERA and down to very small values of x, for all values of Q^2 where the leading twist approximation is applicable.

The failure of the BFKL expansion on the one side and the remarkably accurate description of the HERA data by fixed order perturbation theory on the other, demanded a theoretical explanation. The calculation of three loop splitting functions (NNLO) has made the problem more acute along the way, by showing that at higher orders the fixed order expansion does indeed start to diverge. The solution of the problem is by now well established: important formally subleading terms cannot be ignored and must also be resummed. Their effect is to push the onset of the truly asymptotic regime down to smaller values of x, while in an intermediate region, relevant for HERA data, the evolution shows a shallow dip, somewhat lower than the NLO perturbative result. The resummation procedure is determined by solid guiding principles from duality, momentum conservation, symmetry under gluon exchange of the BFKL kernel and accurate implementation of running coupling effects.

In the present paper, after a summary of the general theoretical principles and methods, we have developed the formalism to the level needed for a direct application to the calculation of physical observables. Resummed splitting functions and coefficients have been evaluated at general values of n_f and α_s and their scheme dependence has been studied in detail, together with a check that this dependence is drastically reduced when the different ingredients are collected together to form physically measurable quantities. Finally we have studied the size of the resulting effects for predictions in the LHC region, showing that their importance while not dramatic is however certainly sizeable, and as big as that of fixed order NNLO terms.

References

[1] S. Moch, J. A. M. Vermaseren and A. Vogt, *Nucl. Phys.* **B691** (2004) 129;
A. Vogt, S. Moch and J. A. M. Vermaseren, *Nucl. Phys.* **B688** (2004) 101.

[2] G. P. Salam, `hep-ph/0607153.`, invited talk at DIS2006 (Tsukuba), Apr 2006.

[3] A. Gehrmann-De Ridder, T. Gehrmann, E.W.N. Glover and G. Heinrich, *Phys. Rev. Lett.* **99** (2007) 132002; *Jour. High Energy Phys.* **0712** (2007) 094.

[4] P.A. Baikov, K.G. Chetyrkin, J.H. Kuhn, `arXiv:0801.1821 [hep-ph]`.

[5] A. Bassetto, M. Ciafaloni and G. Marchesini, Phys. Rept. **100** (1983) 201.

[6] L.N. Lipatov, *Sov. Jour. Nucl. Phys.* **23** (1976) 338;
V.S. Fadin, E.A. Kuraev and L.N. Lipatov, *Phys. Lett.* **60B** (1975) 50; *Sov. Phys. JETP* **44** (1976) 443; **45** (1977) 199;
Y.Y. Balitski and L.N.Lipatov, *Sov. Jour. Nucl. Phys.* **28** (1978) 822.

[7] T. Jaroszewicz, *Phys. Lett.* **B116** (1982) 291.

[8] R. D. Ball and S. Forte, *Phys. Lett.* **B465** (1999) 271.

[9] M. Ciafaloni, D. Colferai, G. P. Salam and A. M. Stasto, *Phys. Rev.* **D66** (2002) 054014; *Phys. Lett.* **B576** (2003) 143; *Phys. Rev.* **D68** (2003) 114003, see also the Proceedings of the HERA-LHC workshop (2005), in press.

[10] M. Dittmar *et al.*, `hep-ph/0511119`.

[11] G. Altarelli, R. D. Ball and S. Forte, *Nucl. Phys.* **B575**, 313 (2000); see also `hep-ph/0001157`.

[12] G. Altarelli, R. D. Ball and S. Forte, *Nucl. Phys.* **B599** (2001) 383; see also `hep-ph/0104246`.

[13] G. Altarelli, R. D. Ball and S. Forte, *Nucl. Phys.* **B621** (2002) 359.

[14] G. Altarelli, R. D. Ball and S. Forte, *Nucl. Phys.* **B674** (2003) 459; see also `hep-ph/0310016`.

[15] G. Altarelli, R. D. Ball and S. Forte, *Nucl. Phys.* **B742** (2006) 1, see also S. Forte, G. Altarelli and R. D. Ball, `hep-ph/0606323`.

[16] G. Salam, *Jour. High Energy Phys.* **9807** (1998) 19.

[17] M. Ciafaloni and D. Colferai, *Phys. Lett.* **B452** (1999) 372.

[18] M. Ciafaloni, D. Colferai and G. P. Salam, *Phys. Rev.* **D60** (1999) 114036; *Jour. High Energy Phys.* **0007** (2000) 054.

[19] M. Ciafaloni, D. Colferai, G. P. Salam and A. M. Stasto, *Phys. Lett.* **B587** (2004) 87; see also G. P. Salam, `hep-ph/0501097`.

[20] R.S. Thorne, *Phys. Rev.* **D64** (2001) 074005;
C.D. White and R.S. Thorne, *Phys. Rev.* **D75** (2007) 034005.

[21] S. Catani, M. Ciafaloni and F. Hautmann, *Phys. Lett.* **B242** (1990) 97; *Nucl. Phys.* **B366** (1991) 135;
J. C. Collins and R. K. Ellis, *Nucl. Phys.* **B360** (1991) 3.

[22] S. Catani and F. Hautmann, *Phys. Lett.* **B315** (1993) 157; *Nucl. Phys.* **B427** (1994) 475.

[23] R. D. Ball and R. K. Ellis, *Jour. High Energy Phys.* **0105** (2001) 053.

[24] R. D. Ball, `arXiv:0708.1277 [hep-ph]`, to be published in *Nucl. Phys.* B.

[25] R. D. Ball and S. Forte, *Phys. Lett.* **B359** (1995) 362.

[26] M. Ciafaloni, D. Colferai, G. P. Salam and A. M. Stasto, `arXiv:0707.1453 [hep-ph]`.

[27] R. Kirschner and L. N. Lipatov, *Nucl. Phys.* **B213** (1983) 122.

[28] R. D. Ball and S. Forte, *Nucl. Phys.* **B742** (2006) 158.

[29] R. D. Ball and S. Forte, *Phys. Lett.* **B405** (1997) 317.

[30] R. D. Ball and S. Forte, *Phys. Lett.* **B351** (1995) 313.

[31] S. Forte and R. D. Ball, AIP Conf. Proc. **602** (2001) 60, `hep-ph/0109235`.

[32] L. N. Lipatov, *Sov. Phys. J.E.T.P.* **63** (1986) 904 [Zh. Eksp. Teor. Fiz. **90** (1986) 1536].

[33] G. Curci, W. Furmański and R. Petronzio, *Nucl. Phys.* **B175** (1980) 27

[34] M. Ciafaloni, *Phys. Lett.* **B356** (1995) 74;
M. Ciafaloni and D. Colferai, *Jour. High Energy Phys.* **0509** (2005) 069;
S. Marzani, R. D. Ball, P. Falgari and S. Forte, *Nucl. Phys.* **B783** (2007) 143.